Phytochem Rev (2025) 24:2271–2307
https://doi.org/10.1007/s11101-024-09964-6

Monoterpene indole alkaloids with anticancer activity from *Tabernaemontana* species

Bruno M. F. Gonçalves · Noélia Duarte · Cátia Ramalhete · Filipa Barbosa · Ana Margarida Madureira · Maria-José U. Ferreira

Received: 15 January 2024 / Accepted: 24 March 2024 / Published online: 27 April 2024
© The Author(s) 2024

Abstract Indole alkaloids, predominantly found in plants, are a large group of natural product-derived compounds characterized by a remarkable chemical diversity associated with significant biological properties. Among these, terpenoid indole alkaloids are the largest group of secondary metabolites. *Tabernaemontana* species (Apocynaceae) are widely distributed in tropical and subtropical regions of the world and used in traditional medicine to treat a variety of illnesses, including tumours. These species biosynthesize large quantities of structurally complex monoterpene indole and bisindole alkaloids. Given the compelling biological properties of indole alkaloids, the phytochemical study of *Tabernaemontana* species has been widely addressed to identify potential anticancer compounds. Several indole alkaloids have shown antiproliferative effect due to different mechanisms, namely by inducing apoptosis or arresting cell cycle, in diverse cancer cell lines, including multidrug-resistant phenotypes. This review primarily aims to underscore the anticancer activity of indole and bisindole alkaloids isolated from several *Tabernaemontana* species. Moreover, our recent contributions to the field are also highlighted, focusing on the study of *Tabernaemontana elegans*. The anticancer evaluation, namely the reversion of P-glycoprotein-mediated multidrug resistance, of two sets of monoterpene indole alkaloid derivatives, obtained by modification of some functional groups of two major monoterpene indole alkaloids, is reviewed, as well as the results obtained for a derivative that targeted homologous recombination DNA repair defects.

Keywords Apocynaceae · *Tabernaemontana* · Monoterpene indole alkaloids · Bisindole indole alkaloids · Cancer · Cytotoxicity · Antiproliferative · Drug resistance

Abbreviations

ABCB1	ATP binding cassette, subfamily B, member 1
BARD1	BRCA1-associated ring domain protein
BRCA1	Breast cancer type 1 susceptibility protein
FAR	Fluorescence activity ratio
IC_{50}	Sample concentration causing 50% inhibition
JNK	C-Jun *N*-terminal kinase
MDR	Multidrug resistance
MTT	3-(4,5-Dimethylthiazol-2-yl)-2,5-diphenyltetrazolium bromide

B. M. F. Gonçalves · N. Duarte · C. Ramalhete · F. Barbosa · A. M. Madureira · M.-J. U. Ferreira (✉)
Faculty of Pharmacy, Research Institute for Medicines (iMed.ULisboa), Universidade de Lisboa, Av. Prof. Gama Pinto, 1649-003 Lisbon, Portugal
e-mail: mjuferreira@ff.ulisboa.pt

C. Ramalhete
ATLÂNTICA – Instituto Universitário, Fábrica da Pólvora de Barcarena, 2730-036 Barcarena, Oeiras, Portugal

PARP Poly (ADP-ribose) polymerase
P-gp P-glycoprotein
ROS Reactive oxygen species

Introduction

Alkaloids are nitrogen-containing compounds that belong to one of the largest groups of natural products and are often linked to significant biological properties. The designation alkaloid (alkali-like) derives from their inherent basic properties, owing to the presence of one or more nitrogen atoms in their structures, commonly in heterocycles. Due to their frequently varied and complex scaffolds, alkaloids are usually classified into diverse classes, such as indoles, quinolines, isoquinolines, pyrrolidines, piperidines, based on their nitrogen-containing structure (Dewick 2009).

In alkaloid biosynthesis, nitrogen atoms predominantly derive from an amino acid precursor, whose carbon skeleton is usually preserved in the alkaloid scaffold in large extension, leading to a different classification (Dewick 2009; Dey et al. 2020).

Terpenoid indole alkaloids constitute the largest subgroup of alkaloids in plants, with many being identified within the Apocynaceae, Loganiaceae, and Rubiaceae families. Monoterpene indole alkaloids have as precursor the amino acid L-tryptophan, whose decarboxylation originates tryptamine, which, generally, reacts with the terpenoid aldehyde secologanin evidenced by a C-9 or C-10 terpenoid moiety incorporated in their structures. According with the rearrangement of the terpenoid part, three main structural types of monoterpene indole alkaloids, namely of the corynanthe, aspidosperma and iboga-type, are formed (Figs. 1 and 2). Coupling reactions between monomeric indole alkaloids give rise to bisindole alkaloids (Dewick 2009).

The genus *Tabernaemontana* belongs to the Apocynaceae family and comprises more than 100 species, distributed as shrubs or small trees in tropical and subtropical regions of the world, including Africa, America, and Asia. Their species are characterised for producing a wide variety of monoterpene indole and bisindole alkaloids with high structural complexity. *Tabernaemontana* species have long been used in traditional medicine, for treating several diseases, including tumours and inflammation (Van Beek et al. 1984; Marinho et al. 2016). Monoterpene indole alkaloids have emerged as pivotal agents in cancer treatment, with compounds such as vinblastine and vincristine (Fig. 3), originally isolated in the 1950s from the Madagascar periwinkle *Catharanthus roseus*. These alkaloids stand as pioneering plant-derived anticancer agents approved for clinical use. Due to their potent cytotoxic activity, new semisynthetic analogous of these alkaloids were prepared and still being in used in clinical settings, namely vinorelbine, vindesine and vinflunine (Fig. 3) (Silvestri 2013; Banyal et al. 2023). Some of these semisynthetic analogues are again in clinical trials to extend their anticancer activity to new types of cancers. In this way, vinorelbine is currently in a phase III trial, for the treatment of patients with rhabdomyosarcoma, a rare type of cancer that may affect mostly the muscles. The aim is to compare its effect when combined with other anticancer agents, including vincristine (Allen-Rhoades 2024). Moreover, the use of vinorelbine as a second-line treatment of malignant pleural mesothelioma, a rare type of cancer that affects the pleura, has also been in a randomised phase II trial (Fennell et al. 2022) (Fennell 2021). Another example of vinca alkaloids that have been the subject of clinical trials against several new types of cancer, namely advanced breast cancer, is the fluorinated derivative vinflunine (Binghe 2019).

In addition, these compounds not only exhibit great structural diversity (O'Connor and Maresh 2006; Song et al. 2023) but also exert their anticancer efficacy through modulation of diverse signalling pathways, encompassing the inhibition of cancer cell proliferation (Kang et al. 2022), cell cycle arrest (Du et al. 2023), and induction of apoptosis (Paterna et al. 2015; Fang et al. 2019). Monoterpene indole alkaloids have also demonstrated therapeutic potential in addressing one of the most challenging obstacles in cancer chemotherapy, the multidrug resistance (MDR) (Cardoso et al. 2021b). This multifactorial phenomenon is characterized by the ability of drug resistant tumours to exhibit simultaneous resistance to several structurally and functionally unrelated chemotherapeutic agents. The development of inhibitors, or modulators, targeting ABC transporters, such as P-glycoprotein (P-gp/ABCB1), multidrug resistance-associated protein 1 (MRP1/ABCC1), and breast cancer resistance protein

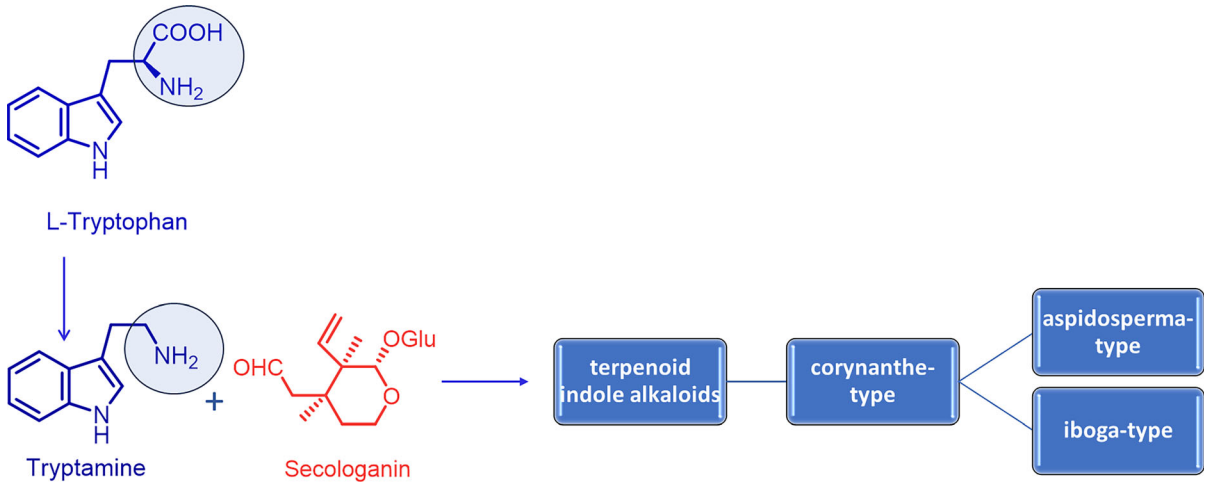


Fig. 1 Terpenoid indole alkaloids are formed from tryptamine, resulting from L-tryptophan, and the terpenoid aldehyde secologanin

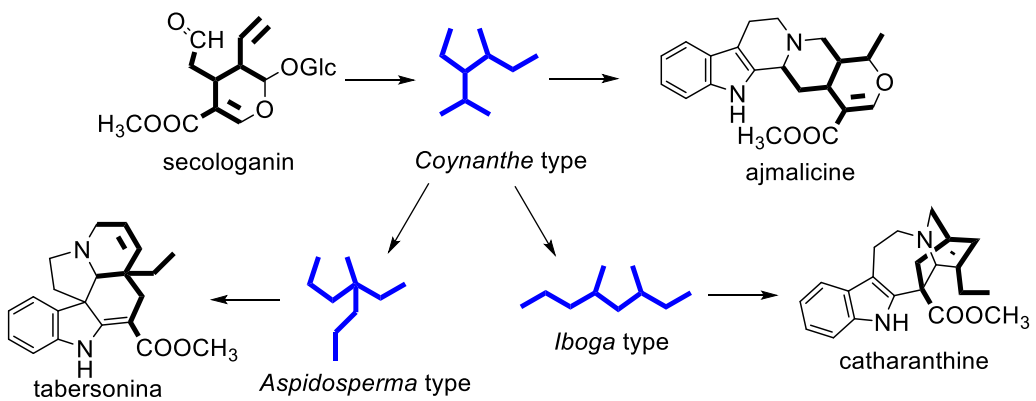


Fig. 2 Rearrangement of secologanin gives rise to three main structural types of terpenoid indole alkaloids, namely of the corynanthe (e.g. ajamalicine), aspidosperma (e.g. tabersonine) and iboga-type (e.g. catharanthine). Adapted from (Dewick 2009)

(BCRP/ABCG2), has been considered a pragmatic strategy for reinstating drug sensitivity in resistant cells when co-administered with anticancer drugs (Feyzizadeh et al. 2022). Another frequently explored approach, known as collateral sensitivity, involves the identification of compounds exhibiting higher cytotoxicity against MDR cells compared to parental cells (Pluchino et al. 2012). Recent investigations have unveiled that monoterpene indole alkaloids and some of their derivatives possess enhanced anticancer properties, namely as selective P-gp (Cardoso et al. 2021a) or MRP1 inhibitors, and with significant collateral sensitivity effect (Paterna et al. 2018). For all these reasons, monoterpene indole alkaloids have been attracting the attention of the scientific community as promising candidates for the development of new anticancer therapeutics.

In this work, the anticancer activity of indole and bisindole alkaloids from *Tabernaemontana* species is reviewed. Aiming at summarizing our contribution in the study of these species, the anticancer evaluation of two sets of monoterpene indole alkaloid derivatives, obtained by modification of some functional groups of two major monoterpene indole alkaloids, isolated from *Tabernaemontana elegans,* is also summarized.

The literature search was performed on Web of Science, ScienceDirect, PubMed, Scopus, and Google Scholar, covering the last four decades of research. Several keyword combinations were utilized, such as *Tabernaemontana*, indole alkaloids, cancer, cytotoxicity, antiproliferative, and multidrug resistance. Only

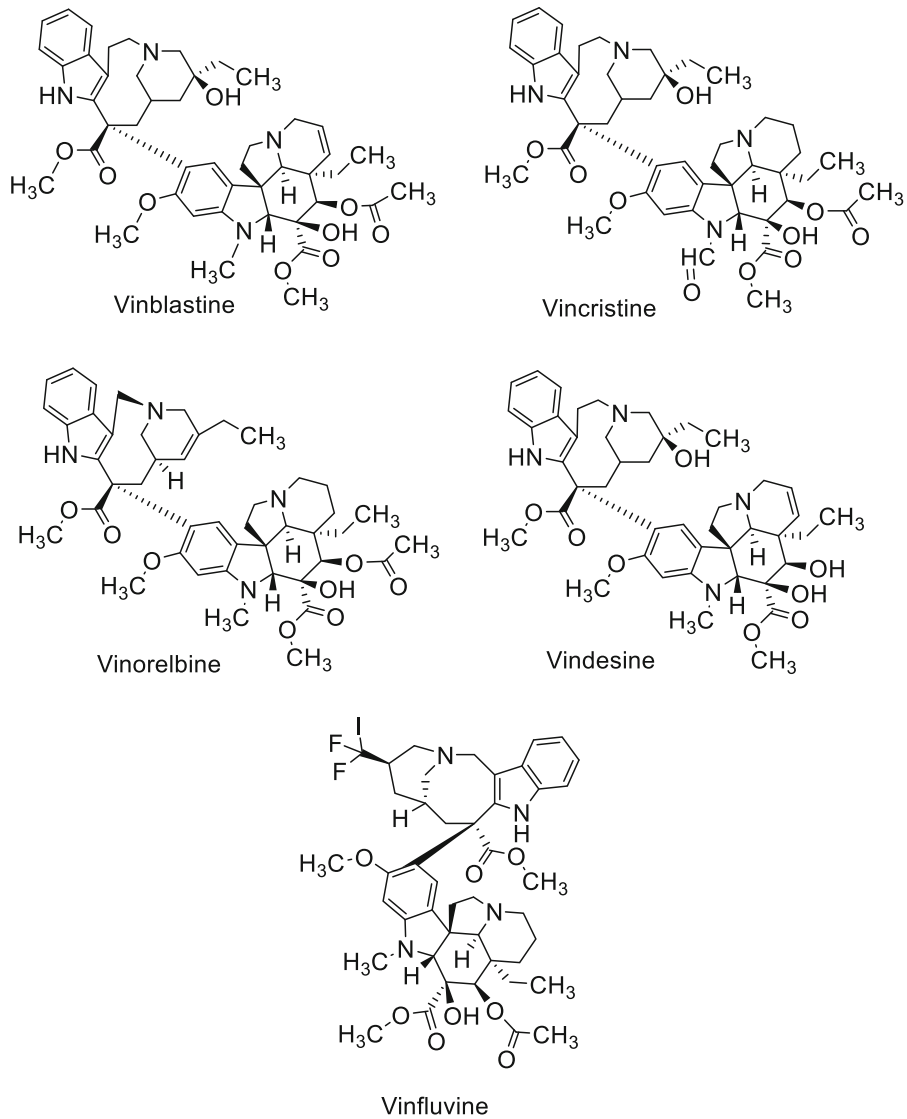


Fig. 3 Examples of some monoterpene indole alkaloids currently employed in clinical settings

peer-reviewed research articles or reviews were considered. Some books and official websites were also accessed. The literature was analysed by the authors, applying as exclusion criteria, poor quality, inaccurate data, and not considered relevant to the aim of the review. Mendeley Reference Manager Software (version 1.19.8, 2020) was used to manage the references and eliminate duplicates.

Indole alkaloids from *Tabernaemontana* genus with anti-cancer activity

Tabernaemontana bovina

T. bovina Lour. (synonym *T. officinalis* Tsiang) is indigenous to Southeast Asian, namely China, Cambodia, Laos, Myanmar, Thailand, and Vietnam. Its roots have been employed in Vietnam traditional medicine to treat fever and jaundice. The aspidosperma-type alkaloid 11-methoxytabersonine (**1**), (Fig. 4), isolated from *T. bovina*, significantly inhibited the viability of two human lung cancer cell lines A549 and H157 (IC_{50} values of 2.68 and 2.02 μM on

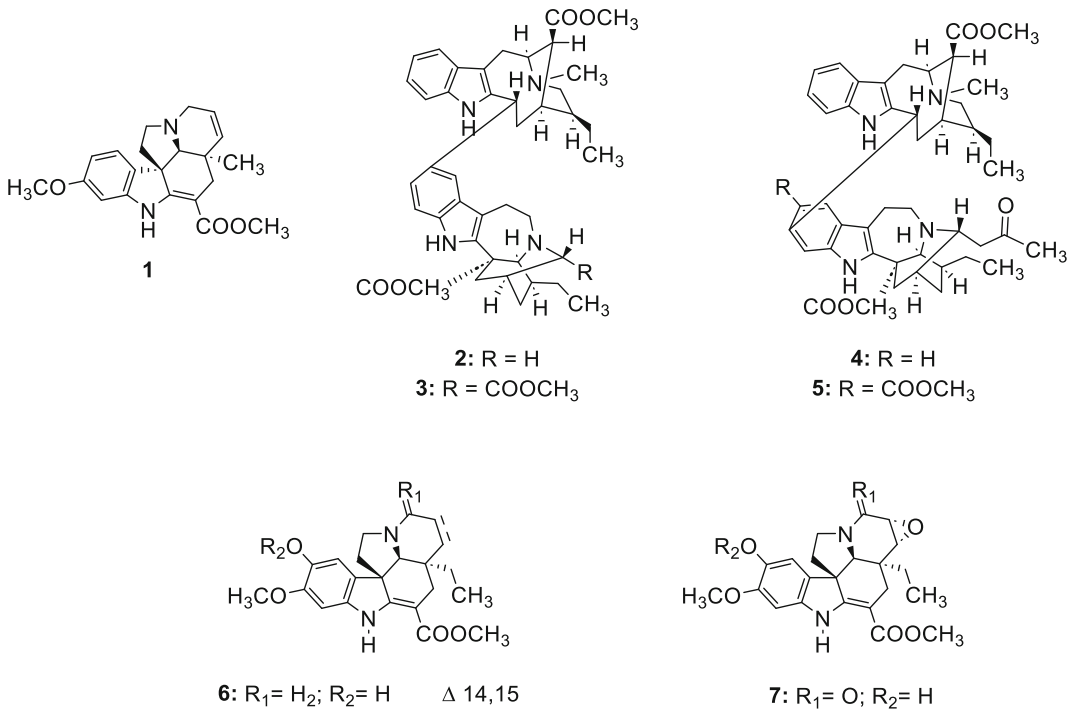


Fig. 4 Chemical structures of compound **1**, taberdivarines C–F (**2**–**5**) and jerantinines A (**6**) and D (**7**) isolated from *T. bovina*

A549 and H157 cells, respectively) (Ge et al. 2020). Similar results were reported by Liu et al. (2012) against a panel of cancer cell lines (Liu et al. 2012). Mechanistic investigations revealed that **1** induced autophagy, which conferred a cytoprotective effect, and concurrently triggered necroptosis rather than apoptosis in the two cell lines. Additionally, the authors have demonstrated that **1** induced autophagy in both cancer cells was caused by its effect on c-Jun *N*-terminal kinase (JNK) and AMP activated protein kinase (Ge et al. 2020). It is important to mention that this compound was firstly isolated from *Melodinus aeneus* (Baassou et al. 1978).

Several novel bisindole alkaloids of the vobasinyl-iboga type, including taberdivarines C–F (**2**–**5**, Fig. 4), were isolated from the leaves and twigs of the species. The cytotoxicity of taberdivarine C-F (**2**–**5**) against human cervical (HeLa), breast (MCF-7), and colorectal (SW480) cancer cell lines was evaluated by the thiazolyl blue tetrazolium bromide (MTT) metabolism assay. All the tested compounds (**2**–**5**) were found to be cytotoxic to the three tested tumour cell lines (IC_{50} values ranging from 1.42 to 11.35 μM), with taberdivarines E (**4**) exhibiting the greatest activity against HeLa and SW480 cancer cell lines, with IC_{50} values of 1.42 and 1.57 μM, respectively. Taberdivarine D (**3**) showed the highest cytotoxic effect on the MCF-7 cell line (IC50 value of 2.84 μM). All of the displayed activities were comparable to those of the positive control, cisplatin. (Zhang et al. 2015a).

The aspidosperma indole alkaloids jerantinines A (**6**) and D (**7**) were isolated from the leaves of *T. bovina* and screened for cells viability inhibition of three hepatoma SMMC-7721, HepG2 and Hep3B cell lines. Both compounds showed similar effects towards SMMC-7721, HepG2 cells with IC_{50} values of 1.66 and 1.33 μM for jerantinine A (**6**) and 1.17 and 1.47 μM for jerantinine D (**7**), respectively. In Hep3B cells, compound **7** proved to be the most active with an IC_{50} value of 1.85 μM versus 5.01 μM exhibited by compound **6**. The activities displayed by both compounds were comparable to that of positive control vinorelbine (IC_{50} values of 3.02, 7.23, 0.60 towards SMMC-7721, HepG2 and Hep3B cells, respectively (Yu et al. 2023).

Tabernaemontana bufalina

Growing in the south of China, *T. bufalina* Lour. (syn. *T. hainanensis* (Tsiang) P.T.Li), which has previously

received most of the research under the name *Ervatamia hainanensis* Tsiang, has been used in traditional Chinese medicine to treat snakebite, rheumatoid arthritis, hypertension, and viral hepatitis. According to phytochemical studies, *T. bufalina* is abundant in indole and bisindole alkaloids, having also diverse lanostane type triterpenes, lignans, and steroids. Among these, certain alkaloids showed notable anti-inflammatory, acetylcholinesterase (AChE) inhibitory and cytotoxic properties (Zhou et al. 2018; Xu et al. 2019). Several monoterpenoid indole alkaloids (**8**–**25**, Fig. 5), including three novel ones, were identified by Zhou et al. from the aerial parts of the plant: 3′-(2-oxopropyl)-19,20-dihydrotabernamine (**8**), 3′-(2-oxopropyl)-ervahanine B (**9**), and 19,20-dihydrovobparicine (**10**) (Zhou et al. 2018).The new compounds together with seven known ones (**11**, **14**, **16**, **17**, **19**, **22**, and **23**) showed cytotoxic activity against a human lung cancer (A-549) and a breast cancer (MCF-7) cell lines with IC_{50} values below 10 μM, being compound **16** the most active in both cell lines (IC_{50} 1.25 μM and 1.19 μM, A-549 and MCF-7, respectively) (Table 1). The cytotoxicity evaluation of compounds was performed by using the sulforhodamine B (SRB) colorimetric assay, being 7-ethyl-10-hydroxy-camptothecin (SN38) used as a positive control (Zhou et al. 2018).

Conophylline (**24**), a bisindole alkaloid isolated from the same plant's branches and leaves, exhibited cytotoxic activity against the murine skin melanoma cell line B16 and the human breast cell line MDA-MB-231 cell lines (IC_{50} values of 0.13 and 8.9 μM, respectively) (Xu et al. 2019). The IC_{50} value on B16 cells was 68 times lower than that on MDA-MB-231 cells, revealing a significant level of selective cytotoxicity for the B16 cell line (Xu et al. 2019). Gambogic acid (IC_{50} values of 22.1 and 13.5 μM on B16 and MDA-MB-231 cells, respectively) was used by the authors as a positive control (Xu et al. 2019). Other indole alkaloids isolated, including the new undescribed monoterpenoid indole alkaloid (3*R*,7*S*,14*R*,19*S*,20*R*)-19-hydroxypseudovincadifformine (**25**), did not exhibit cytotoxic effect on the tested cells ($IC_{50} > 100$ μM)(Xu et al. 2019).

The phytochemical investigation on the aerial parts of *T. bufalina* led to the identification of the ibogabobasine bisindole vobatensine C (**26**). When evaluated for its toxicity against A-549 human lung adenocarcinoma, Bel-7402 human hepatoma and HCT-116 human colon cancer cell lines, this compound showed significant bioactivity with IC_{50} values of 2.61, 1.19, and 1.74 μM, respectively (5-fluorouracil, with IC_{50} values of 0.80, 1.78 and 1.59 μM was used as control)(Chen et al. 2022).

Tabernaemontana catharinensis

T. catharinensis A. DC. is an arboreal species found in South America, namely Argentina, Paraguay, Bolivia, and Brazil. It is locally known as "corbina" and "forquilheira" in Rio Grande do Sul, Brazil. Traditionally, indigenous population uses this plant as an anticancer therapy. Beyond its anticancer activities, *T. catharensis* extracts have demonstrated antiparasitic, antiophidic, anti-inflammatory, anti-malarial, and anticholinesterase properties. These effects are attributed to the presence of indole alkaloids (Rosales et al. 2019; Reis et al. 2022).

From the stem bark of the plant four known alkaloids were isolated (Fig. 6, 27–30) (Reis et al. 2022). Their in vitro antiproliferative activity was screened on several tumour cell lines, showing affinisine (**29**) the best activity against all the cell lines tested, namely glioma (U251, GI_{50} 9.5 μM), multidrug resistant ovarian adenocarcinoma (NCI-ADR/RES, GI_{50} 8.3 μM), renal adenocarcinoma (786–0, GI_{50} 8.3 μM), and colorectal adenocarcinoma (HT29, GI_{50} 9.3 μM) cell lines (Table 2). Apopvincaminate (**28**) and voachalotine (**30**) were inactive in all cell lines, while voacangine (**27**) showed a moderate antiproliferative effect against the colorectal adenocarcinoma (HT29, GI_{50} 14.4 μM) (Reis et al. 2022).

Tabernaemontana corymbosa

T. corymbosa (Roxb. ex Wall.) has a widespread distribution in the tropical and subtropical regions of Africa, America and Asia and possesses a vast application in traditional medicine.

Practically almost all parts of the plant, which include fruits, leaves, sap, latex, stem bark, root bark, and whole plant are employed as poultice, boiled juice, decoctions and infusions for treatment of several illnesses, including ulceration, fracture, postnatal recovery, syphilis, fever, orchitis and tumours in countries such as Malaysia, China, Thailand and Bangladesh (Abubakar and Loh 2016). Due to this

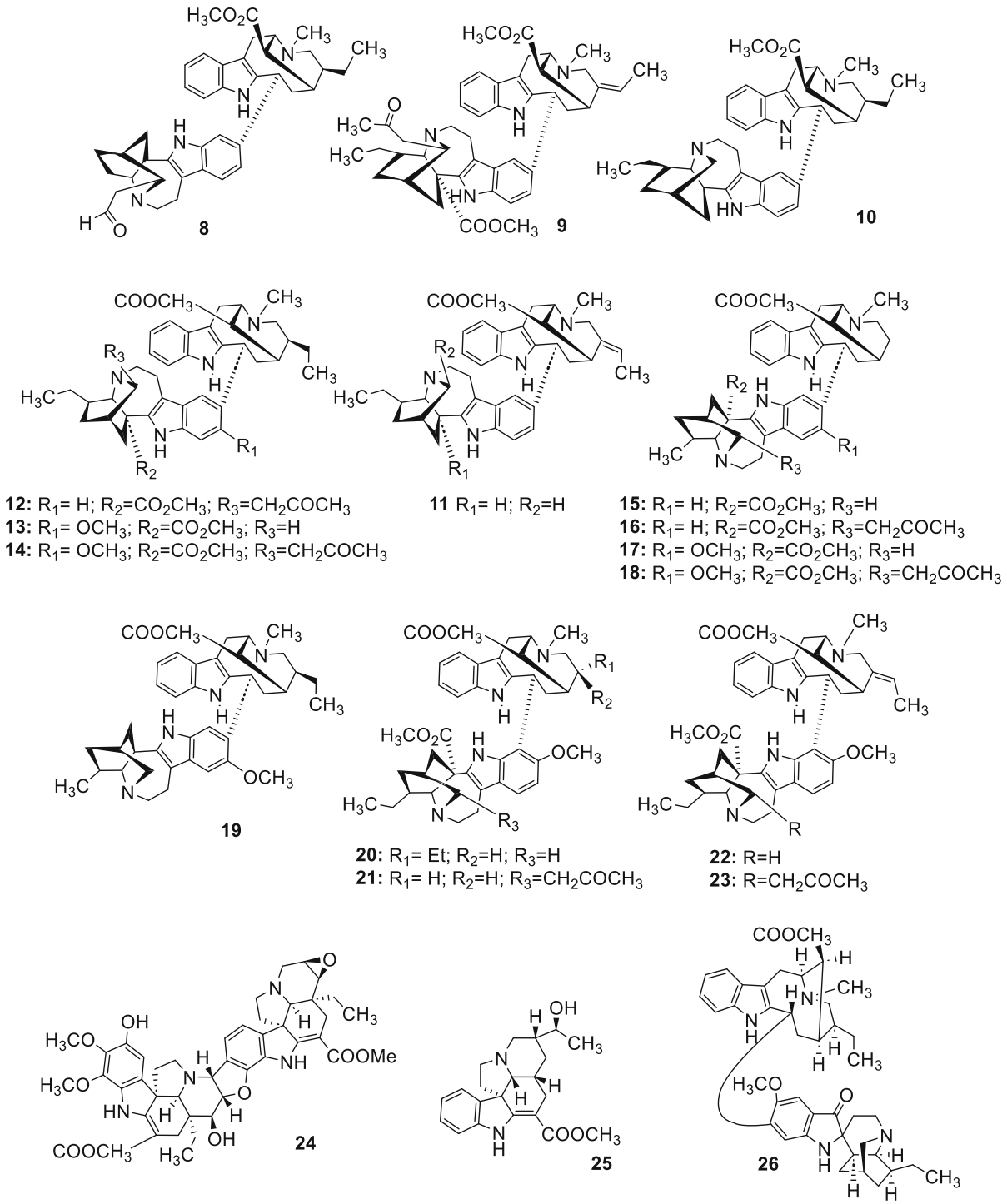


Fig. 5 Chemical structures of alkaloids **8**–**26** isolated from *T. bufalina*

reported pharmacological activities *T. corymbosa* has attracted interest among the scientific community, who have sought novel compounds to fight cancer. Among the array of compounds found in this plant, indole alkaloids have emerged as predominant and well-explored phytochemicals. However, it should be

Table 1 Cytotoxicity of compounds **8–23** (IC_{50}, μM) against MCF7 (breast, adenocarcinoma) and A549 (human lung cancer cells) (Zhou et al. 2018)

	Cell Line[a]/IC_{50} μM			Cell Line[a]/IC_{50} μM	
Compound	MCF7	A549	Compound	MCF7	A549
8	3.07	4.78	**17**	3.40	3.38
9	2.15	4.15	**18**	3.55	19.49
10	3.63	2.52	**19**	1.44	4.24
11	1.38	2.12	**20**	10.87	14.53
12	13.97	37.95	**21**	12.95	23.82
13	3.41	10.08	**22**	3.91	5.42
14	3.73	3.72	**23**	6.13	5.19
15	5.37	31.72	**SN38**	< 0.1	0.24
16	1.25	1.19			

[a]Human cancer cell lines: MCF7 (breast adenocarcinoma) and A549 (lung adenocarcinoma). SN38 (7-ethyl-10-hydroxy-camptothecin): positive control

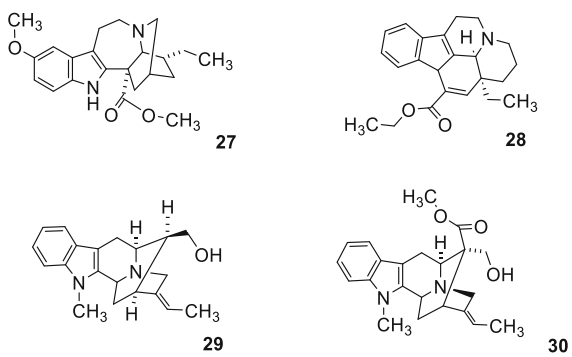


Fig. 6 Chemical structures of compounds **27–30** isolated from *T. catharinensis*

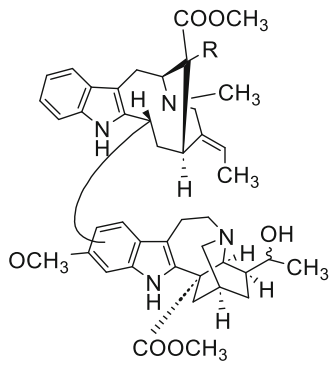
underscored that the geographic location and collection time can significantly influence the alkaloids profile of this plant (Lim et al. 2015). Furthermore, it is essential to acknowledge that *T. corymbosa* has been included on the International Union for Conservation of Nature list of threatened species (Smedley et al. 2018), which raises concerns about the sustainable supply of these promising metabolites.

As far as we know, the earliest report on indole alkaloids from *T. corymbosa* with potential in cancer treatment dates back to 1998, when Kam et al. (1998) isolated the dimeric vobasine-iboga bisindole conodiparines A–D (**31–34**, Fig. 7) from the plant leaves (Kam et al. 1998). All four compounds underwent screening to evaluate their capability in reversing multidrug resistance in vincristine-resistant human oral epidermoid KB cells. Results unveiled that while the compounds exhibited reduced toxicity against both sensitive (IC_{50} 25.6–28.6 μM) and resistant (IC_{50} 18.0–22.7 μM) KB cells individually, their concomitant treatment with 0.30 μM of vincristine (a concentration that did not affect the growth of the KB/VJ300 cells) substantially augmented their cytotoxic effects, leading to a IC_{50} value of 1.9 μM for compound **31** (Kam et al. 1998). Although the mechanisms underlying this action remain undisclosed, the observed effect underscored the necessity for further exploration of conodiparines A–D (**31–34**), particularly concerning their potential as multidrug resistance reversal agents and whether the increased activity in combination with vincristine was attributed to an additive or synergistic effect.

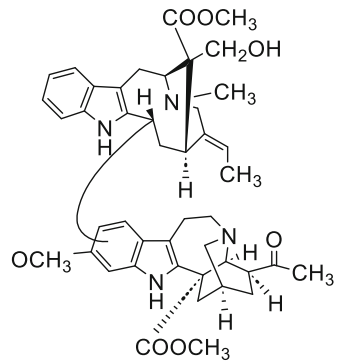
Table 2 Antiproliferative activity of compounds **27–30** (IC_{50}, μM) (Reis et al. 2022)

	Cell Line[a]/IC_{50} μM					
Compound	U251	MCF7	NCI-ADR/RES	786–0	HT-29	NCI-H
Voacangine (**27**)	67.8	40.5	29.6	44.5	14.4	42.7
Apopvincaminate (**28**)	< 100	< 100	53.0	< 100	< 100	< 100
Affinisine (**29**)	9.5	17.1	8.3	8.3	9.3	13.1
Voachalotine (**30**)	< 100	< 100	< 100	< 100	< 100	< 100
Doxorubicin	0.06	0.046	0.6	0.1	0.39	0.046

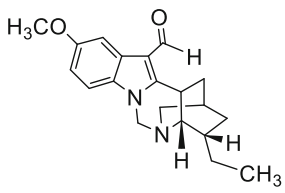
[a]Human tumour cell lines: U251 (glioblastoma); MCF7 (breast adenocarcinoma); NCI-ADR/RES (multi-drug resistant ovarian adenocarcinoma); 786–0 (kidney adenocarcinoma); NCI-H460 (lung large cell carcinoma); HT-29 (colon adenocarcinoma)



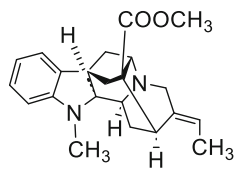
31: R_1= CH_2OH, 19' (*S*), C(3)-C(10') bond
32: R_1= CH_2OH, 19' (*S*), C(3)-C(12') bond



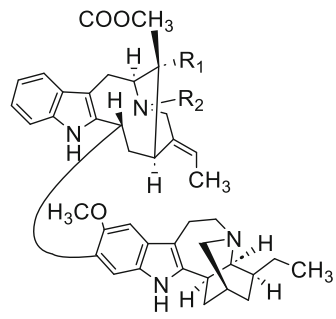
33: C(3)-C(10') bond
34: C(3)-C(12') bond



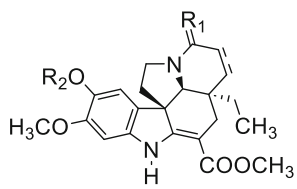
35



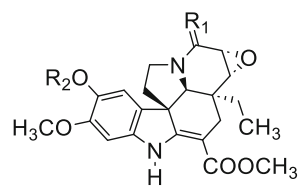
36



37: R_1= CH_2OH; R_2= CH_3
38: R_1= R_2= H



6: R_1= H_2; R_2= H Δ 14,15
40: R_1= O; R_2= H Δ 14,15
41: R_1= H_2; R_2= H
42: R_1= H_2; R_2= $COCH_3$



39: R_1= H_2; R_2= H
7: R_1= O; R_2= H
43: R_1= H_2; R_2= $COCH_3$

Fig. 7 Chemical structures of conodiparines A–D (**31**–**34**), lirofoline A (**35**), vincamajicine (**36**), ervantensines A (**37**) and B (**38**), jerantinines A–E (**6**, **39**, **40**, **7**, **41**), jerantinine A acetate (**42**) and jerantidines B acetate (**43**) isolated from *T. corymbosa*

Lirofoline A (**35**), a rare alkaloid characterized by a rearranged ibogan ring system, presented outcomes analogous to those observed with conodiparines (**31**–**34**). It exhibited diminished cytotoxicity against both drug-sensitive and vincristine-resistant KB cells. Notably, when co-administered with vincristine at a concentration of 0.12 μM, lirofoline A (**35**), effectively restored vincristine sensitivity in KB cells with vincristine resistance (VJ300) (Low et al. 2010).

The repertoire of alkaloid structures exhibiting drug resistance reversal properties was later expanded by the inclusion of the indole vincamajicine (**36**) and the vobasinyl-iboga bisindole alkaloids, ervatensines A (**37**) and B (**38**) isolated from the stem-bark (Lim et al.

2015). While vincamajicine (**36**) demonstrated drug resistance reversal activity solely in vincristine-resistant KB cells when used in combination with 0.12 μM vincristine (a concentration that did not affect the growth of the KB/VJ300 cells), ervatensines A (**37**) and B (**38**) displayed significant growth-inhibitory effects against both drug-sensitive (IC_{50} 0.95–0.53 μM) and vincristine-resistant KB cells (IC_{50} 0.98–1.11 μM) (Table 3). Unfortunately, reports detailing the underlying mechanism of this effect remain elusive. Moreover, compounds **37** and **38** exhibited robust growth-inhibitory activity against several human cancer cell lines (IC_{50} 0.70–4.19 μM) (Table 4). Insights from cell cycle and annexin V-FITC apoptosis assays indicated that compounds **37** and **38** arrested proliferation in human colorectal carcinoma HCT-116 and estrogen-intensive human breast adenocarcinoma MDA-MB-468 cells, inducing apoptotic and necrotic cell death (Lim et al. 2015).

Some of the most intriguing compounds sourced from the plant leaves are the aspidosperma indole alkaloids, specifically jerantinines A–E (**6**, **39**, **40**, **7**, **41**, respectively). These compounds displayed pronounced cytotoxicity against both vincristine-sensitive (IC_{50} 0.68–2.65 μM) and -resistant (IC_{50} 0.95–2.03 μM) human KB cells, an unusual feature among simple aspidosperma alkaloids (Table 4). Furthermore, structural modifications, such as the acetylation of the free hydroxyl group in jerantinines A (**6**) and B (**39**) to yield derivatives **42** and **43**, showed to be beneficial for the cytotoxicity, with IC_{50} values ranging from 0.70–1.04 μM (KB/S) and 0.75–83 μM (KB/VJ300) (Lim et al. 2008).

The exceptional properties of jerantinines swiftly attracted the interest of medicinal chemists. In that way, in 2013 Jérôme Waser et al. developed a method for the total synthesis of jerantinine E (**41**), involving 17 steps with a 16% overall yield. Subsequent in vitro assessments revealed that jerantinine E (**41**) displayed relevant cytotoxic effects on breast (MCF-7) and lung (A549 and HTB-178) cell lines, attaining IC_{50} values as low as 1 μM in A549 cells. Additionally, this compound was found to inhibit cell migration in all four cell lines, reducing it by 50–90% compared to untreated cells. Preliminary studies into its mechanism of action suggested that jerantinine E (**41**) disrupts the microtubule network, thus inhibiting tubulin polymerization (Frei et al. 2013).

The total synthesis of jerantinine A (**6**) was also developed (Smedley et al. 2018). Subsequent investigations led by Bradshaw and co-workers, entailed the evaluation of jerantinines A (**6**) and B (**39**) alongside their acetylated derivatives **42** and **43** towards additional cancer cell lines derived from colorectal (HCT-116, HT-29), breast (MCF-7, MDA-468) and lung (A549) carcinomas. Notably, these compounds consistently exhibited potent cytotoxic activities with IC_{50} values ranging from 0.26 to 3.74 μM. In general, compound **39** showed higher activity than **6** in the tested cell lines, suggesting that the epoxide moiety of **39** may confer enhanced potency. Interestingly, the acetate derivatives of jerantinines A (**42**) and B (**43**)

Table 3 Cytotoxicity of compounds **31–38**

Compound	Cell Line[a]/IC_{50} μM			Ref.
	KB/S	KB/VJ300	KB/VJ300[b]	
Conodiparine A (**31**)	25.6	18.0	1.9	Kam et al. (1998)
Conodiparine B (**32**)	27.7	19.9	3.2	Kam et al. (1998)
Conodiparine C (**33**)	28.6	22.7	7.5	Kam et al. (1998)
Conodiparine D (**34**)	24.9	18.2	6.1	Kam et al. (1998)
Lirofoline A (**35**)	–	–	10.48	Low et al. (2010)
Vincamajicine (**36**)	> 50	> 50	2.62	Lim et al. (2015)
Ervatensine A (**37**)	0.95	1.11	1.20	Lim et al. (2015)
Ervatensine B (**38**)	1.53	0.98	0.80	Lim et al. (2015)

[a]KB/S and KB/VJ300 are vincristine-sensitive and resistant human oral epidermoid cell lines respectively. IC_{50} values were determined by MTT assay following 72 h exposure of cells to test agents ($n \geq 3$). [b]With added vincristine 0.30 μM (Kam et al. 1998) or 0.12 μM (Lim et al. 2015), which did not affect the growth of the KB/VJ300 cells

Table 4 Cytotoxicity of compounds **6**, **7**, **37**–**43**[a]

Compound	Cell Line/IC_{50} (μM)											Ref.
	KB/S	KB/VJ300	MDA-MB-468	MCF-7	HCT-116	VR HCT-116	HT-29	A549	HTB-178	MIA PaCA-2	MRC-5	
Ervatensine A (**37**)	1.39	1.21	2.77	4.19	2.91	–	2.57	3.06	–	–	–	Lim et al. (2015)
Ervatensine B (**38**)	0.95	1.11	0.70	4..23	2.03	–	1.58	2.83	–	–	–	Lim et al. (2015)
Jerantinine A (**6**)	1.99	1.73	0.80	0.85	0.76	0.44	2.52	3.74	–	–	–	Lim et al. (2008) Raja et al. (2014) Qazzaz et al. (2016)
Jerantinine B (**39**)	1.11	0.95	0.39	1.94	0.71	0.49	0.63	0.58	–	0.25	1.92	Lim et al. (2008) Raja et al. (2014) Qazzaz et al. (2016)
Jerantinine C (**40**)	0.81	1.54	–	–	–	–	–	–	–	–	–	Lim et al. (2008)
Jerantinine D (**7**)	0.68	0.95	–	–	–	–	–	–	–	–	–	Lim et al. (2008)
Jerantinine E (**41**)	2.55	2.03	–	5.19	–	–		1.00	2.33	–	–	Lim et al. (2008)Frei et al. (2013)
JA Acetate (**42**)	1.04	0.83	0.38	0.86	0.69	–	2.74	0.79	–	–	–	Lim et al. (2008) Raja et al. (2014)
JB Acetate (**43**)	0.70	0.75	0.26	0.48	0.36	0.36	0.65	0.89	–	0.25	–	Lim et al. (2008) Raja et al. (2014) Qazzaz et al. (2016)
Vincristine	–	–	–	–	0.005	1.34	–	–	–	–	–	Qazzaz et al. (2016)

[a]KB/S and KB/VJ300 are vincristine-sensitive and resistant human oral epidermoid cell lines respectively. MTT assay, following 72 h exposure of cells to test agents. Mean ± SD IC_{50} values (μM) are values from ≥ 3 independent trials

possessed enhanced potency across most of the tested cell lines when compared to their parent compounds, specially compound **43**, which depicted an IC_{50} lower than 1 μM in all cell lines (Raja et al. 2014). However, in clonogenic assays, a disparity emerged when the acetylated derivative **43** was compared with jerantinine B (**39**); jerantinine B acetate (**43**) showed reduced potency toward HCT-116 and MCF-7 after 24-h treatment period. These results suggested that the acetate derivative may act as a prodrug reliant on bioactivation by cellular esterases (Qazzaz et al. 2016).To shed some light on the mechanism of action, the authors focused on jerantinine A (**6**) for additional studies. This compound inhibited the HCT-116 and HT-29 cell colony formation and precipitated a profound cell cycle arrest at G2/M phase across all cell lines. Analogous to the action of jerantinine E (**41**), the cell cycle blockage by jerantidine A (**6**) was apparently related with the inhibition of tubulin polymerization. This inhibition perturbs the dynamic microtubule network, thereby preventing successful mitosis. The presence of aneuploidy and the down-regulation of cyclin B1 supported these conclusions. In addition, the mode of action of this compound seemed to involve an apoptotic process of cell death subsequent to the cell cycle arrest (Raja et al. 2014). However, considering that the therapeutic potential of anti-microtubule and tubulin polymerization drugs such as vinblastine and paclitaxel is often constrained by phenomena such as drug resistance, toxicity and limitations in intravenous delivery, a similar output was anticipated for jerantinine A (**6**). Therefore, to overcome these limitations, Abubakar and co-workers envisioned a combination strategy. In this approach, jerantinine A (**6**) was concomitantly administered with γ-tocotrienol, a vitamin E isomer with pronounced in vitro anticancer activity (Abubakar et al. 2017). At low concentrations (3.14 μM for γ-tocotrienol and 0.42 μM for **6**), this combination induced a potent antiproliferative effect on human glioblastoma

(U87MG) cells. The combination index (CI) of 0.67 suggested a potential synergistic pharmacological effect ($CI < 1$). Treatment with these combined compounds also induced a G0/G1 cell cycle arrest, in contrast to the G2/M arrest observed when jerantinine A (**6**) was applied alone. On the other hand, both the combination and **6** alone led to the disruption of microtubule networks by triggering Fas- and p53-induced apoptosis, mediated via death receptor and mitochondrial pathways. The more relevant finding of this study was the observation of reduced undesirable toxicity to MRC5 non-tumoural fibroblasts when jerantinine A (**6**) and γ-tocotrienol were administered in combination. These outcomes underscore the therapeutic potential of this combination, achievable at lower individual doses, thereby mitigating the potential toxicity of jerantinine A (**6**) and surmounting the high-dose limitations of γ-tocotrienol (Abubakar et al. 2017). Furthermore, jerantinine A (**6**) also was found to induce tumour specific cell death in breast cancer cells by modulating splicing factor 3b subunit 1 (SF3B1), giving rise to abnormal splicing patterns that culminate in apoptosis (Chung et al. 2017). The precise mechanism by which jerantinine A (**6**) interferes with splicing activity remains to be elucidated. Nonetheless, these findings underscore jerantinine A's multi-targeted and tumour-specific nature, rendering it an appealing candidate for future development.

Jerantinine B (**39**) and its acetylated derivative (**43**) were also deeper explored by evaluating their activity against additional cancer cells, including MIA PaCa-2 (pancreatic) and vincristine resistant (VR) HCT-116 cells, as well as non-tumoural MRC5 fibroblasts. MIA PaCa-2 cells showed high sensitivity to both **39** and **43** with IC_{50} values of 0.25 μM. Interestingly, jerantinine B (**39**), as well as jerantinine A (**6**), exhibited activity against vincristine resistant HCT-116 cells expressing P-gp protein, featuring IC_{50} values of 0.44 and 0.49 respectively, which were lower than those observed for sensitive HCT-116 cells. Preliminary mechanistic studies unveiled that, in addition to the time- and dose-dependent induction of apoptosis, cell cycle arrest at G2/M phase and inhibition of tubulin polymerization, akin to analogues jerantinine A (**6**), jerantinine B (**39**) also triggered a substantial increase in the level of reactive oxygen species (ROS). This induction of ROS production may be correlated with the observed release of cytochrome c and caspase activation, preceding cellular apoptosis. Jerantinine B (**39**) was found to inhibit the activity of kinases involved in mitosis and significantly evoked potent G2/M cell cycle arrest with PLK1 being targeted in a dose-dependent manner (Qazzaz et al. 2016). Moreover, a synergistic pharmacological effect between jerantinine B (**39**) and δ-tocotrienol was observed in U87MG and HT-29 cells when both compounds were administered concomitantly, exhibiting CI values of 0.85 and 0.77 for U87MG and HT-29 cells, respectively. This resulted in up to a twofold and 3.8-fold dose reduction of δ-tocotrienol and jerantinine B (**39**), respectively (Abubakar et al. 2016). The anticancer effect of jerantinine B (**39**) was further validated towards acute myeloid leukaemia (AML), a heterogenous hematological malignancy with poor long-term survival. AML cell lines and patient samples exposed to jerantinine B (**39**) displayed significantly impaired cell growth in a dose-dependent manner, accompanied by an early-induced apoptotic cell death (occurring as early as 4 h after treatment). Studies on the mechanism of action suggested that effect of jerantinine B (**39**) in AML cells was associated with the induction of oxidative stress, particularly mitochondrial release of ROS, which subsequently triggered the activation of the c-Jun/JNK signalling pathway (Alhuthali et al. 2020). It is important to note that early activation of JNK has been reported as a specific mechanism mediating microtubule depolymerization and G2/M arrest (Chen et al. 2012). Finally, X-ray crystallography studies of the tubulin—(−)-jerantinine B acetate (**43**) complex demonstrated that this compound binds at the colchicine site resulting in microtubule disruption (Smedley et al. 2018). These collective findings underscore the potential of jerantinine B (**39**) and its acetylated derivative (**43**) to behave as potential multitarget anticancer agents (Table 5).

A series of 10 new indole alkaloids, tabercarpamines A − J, were isolated from the leaves of *T. corymbosa*. Within this set of compounds, only tabercarpamines A (**44**) and B (**45**) (Fig. 8), demonstrated noteworthy cytotoxic activities against human hepatocellular (SMMC-7721 and Hep-G2) and breast (MCF-7) carcinoma cell lines. Remarkably, compound **44** exhibited higher activity than cisplatin towards both hepatocellular cancer cell lines. Consequently, the authors extended their investigation into the anti-cancer properties of tabercarpamine A (**44**) in HepG2 cells to elucidate its mechanism of action, and the results revealed that the cytotoxicity might be

Table 5 Relevant activities of jerantinines A (**6**), B (**39**), E (**41**), and jerantinine B acetate (**43**)

Compound	Tumour type	Cell line	Activity/Targets	Ref.
Jerantinine E (**41**)	Breast	MCF-7 and MDAMB-231	Inhibition of cell migration	Frei et al. (2013)
	Lung	A549	Disruption of the microtubule network; Inhibition of the tubulin polymerization	
Jerantinine A (**6**)	Colon	HCT-116, HT-29	G2/M cell cycle arrest Inhibition of tubulin polymerization and microtubule disruption (↓ Cyclin B1)	Raja et al. (2014)
	Lung	A549		
	Breast	MCF-7	Induction of apoptosis (↑PARP, ↑ Cleaved caspase 3, ↓BCL-2, ↓Mcl-1, ↓ Hdm2 and ↑ p53)	
	Brain	U87MG	**In combination with γ-tocotrienol:** Pharmacological synergistic effect G0/G1 cell cycle arrest Disruption of microtubule networks Induction of apoptosis (↑ p53, ↑p27, ↑Fas, ↑Bid, ↑ Cyt *c*)	Abubakar et al. (2017)
	Breast	MCF-7 T47D MDA-MB-468	Tumour-specific cell death in breast cancer cell lines Induction pre-mRNA splicing errors-modulation of slicing Induction of apoptotic cell death Upregulation of SF3B1 and SF3B3 proteins	Chung et al. (2017)
Jerantinine B (**39**)	Colon	HCT-116	Cell Cycle arrest at G2/M phase (↓ PLK1) Inhibition of tubulin polymerization increases in reactive oxygen species (ROS) Apoptosis induction (↑- Cleaved PARP, ↑ Cleaved caspase 3/7, ↓ Blc-2, ↓Mcl-1)	Qazzaz et al. (2016)
	Lung	A549		
	Pancreas	MIA PaCa-2		
	Blood-Leukaemia	MV4–11 HL-60	Apoptosis induction (↑ cleaved caspase 3, ↑cleaved PARP) Induction of c-Jun/JNK activation Induction of ROS production	Alhuthali et al. (2020)
Jerantidine B acetate (**43**)	Crystal structure of the tubulin-jerantinine B acetate (9) complex	Binds to the colchicine site of tubulin blocking the tubulin polymerization		Smedley et al. (2018)
	Blood-Leukaemia	Primary patient cells	Dose- dependent inhibition of colony formation	Alhuthali et al. (2020)

PARP Poly (ADP-ribose) polymerase, *Hdm2 -; Fas* Apo 1/CD 95/tumour necrosis factor superfamily 6, *Cyt c* Cytochrome c, *SF3B1* splicing factor 3b subunit 1, *SF3B3* Splicing factor 3b Subunit 3, *PLK1*- Polo-like kinase 1, *Blc-2* B-cell lymphoma 2, *Mcl-1* Myeloid leukaemia 1 antiapoptotic protein, *c-Jun/JNK* c-Jun N-terminal kinases

related with its ability to induce apoptosis (Ma et al. 2014).

Four new vobasinyl-ibogan type bisindole alkaloids, tabercorines A–C (**46**–**48**) and 7-acetyltabernaecorymbosine A (**49**) (Fig. 8) were tested for their in vitro cytotoxicity against human leukaemia (HL-60), hepatocarcinoma (SMMC-7721), lung (A549), breast (MCF-7) and colorectal (SW480)

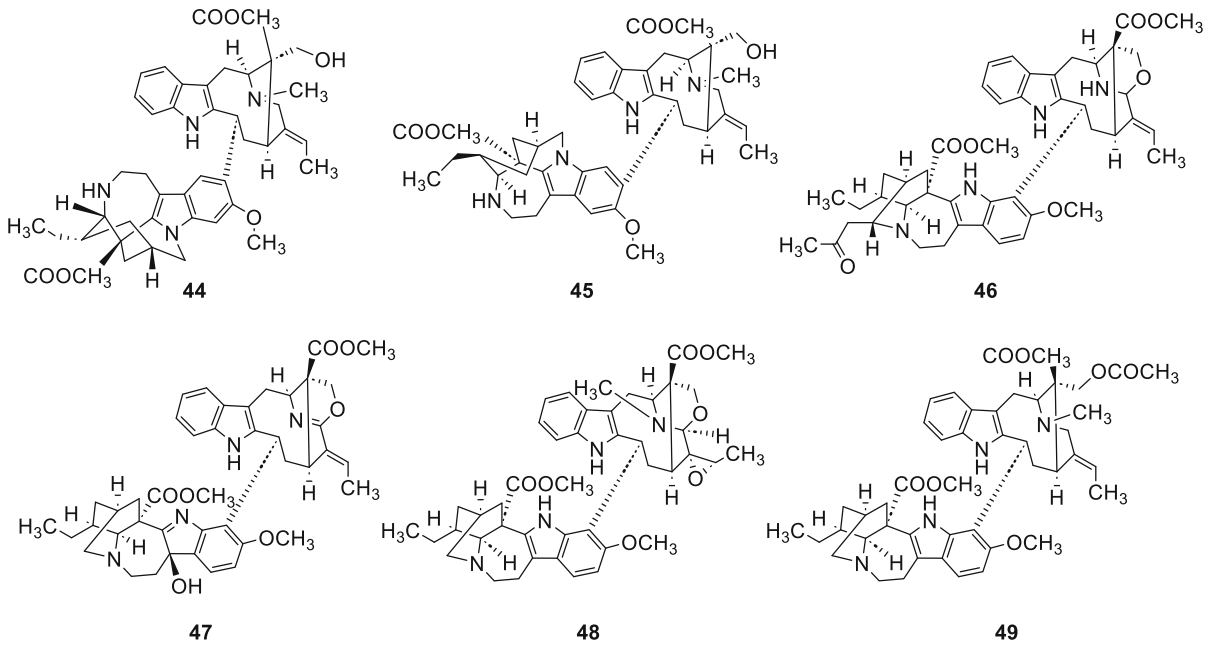


Fig. 8 Chemical structures of tabercarpamine A (**44**), tabercarpamine B (**45**), tabercorines A–C (**46–48**) and 7-acetyl-tabernaecorymbosine A (**49**)

cancer cell lines. No interesting inhibitory effects were observed for compound **48** (IC_{50} ranging from 14.95 to > 40 μM). Tabercorine B (**47**) on the other hand exhibited moderate cytotoxic activity (IC_{50} ranging from 4.70 to 16.93 μM), especially towards breast cancer cells (Zhang et al. 2015b). Subsequent studies further confirmed the anticancer potential of tabercorine B (**47**) with IC_{50} values ranging from 4.5 to 8.2 μM in several cell lines (Zhang et al. 2018b). However, the most compelling findings were associated with tabercorine A (**46**) and 7-acetyl-tabernaecorymbosine A (**49**), which displayed strong inhibitory properties (IC_{50} ranging from 2.98 to 9.24 μM for compound **46** and IC_{50} ranging from 2.90 to 4.75 μM to compound **49** comparable to those of the reference drug cisplatin (IC_{50} 1.05–13.13 μM) (Zhang et al. 2015b) (Table 6).

Table 6 Cytotoxicity of bisindole alcaloids tabercarpamines A (**44**) and B (**45**), tabercorines A -C (**46–48**) and 7-acetyl-tabernaecorymbosine (**49**)

Compound	Cell Line/IC_{50} (μM)[a]						Ref.
	Hep-G2	**HL-60**	**SMMC-7721**	**A-549**	**MCF-7**	**SW480**	
Tabercarpamine A (**44**)	3.31	–	6.76	–	8.54	–	Ma et al. (2014)
Tabercarpamine B (**45**)	11.26	–	14.96	–	10.92	–	Ma et al. (2014)
Tabercorine A (**46**)	–	2.98	3.53	4.14	8.10	9.24	Zhang et al. (2015b)
Tabercorine B (**47**)	–	14.79	13.31	10.34	4.70	16.93	Zhang et al. (2015b)
Tabercorine C (**48**)	–	14.95	31.52	33.16	> 40	> 40	Zhang et al. (2015b)
7-acetyl-tabernaecorymbosine A (**49**)	–	2.90	4.67	3.83	4.75	4.70	Zhang et al. (2015b)
Cisplatin	–	1.05	4.46	6.57	13.13	11.07	Zhang et al. (2015b)

[a]Hep-G2: Human liver cancer; HL-60: Human promyelocytic leukaemia; SMMC-7721- human hepatocellular carcinoma_ A-549: human lung cancer; MCF-7: Human breast cancer; SW480: human colorectal adenocarcinoma cell lines. The different cell lines were treated with crescent concentrations of each compound for 48 h. IC50 values were determined using MTT method. Mean IC_{50} values (μM) are values from ≥ 3 independent assays; IC_{50} is the concentration of compound that inhibits 50% of cell growth

Additionally, several other bisindole alkaloids demonstrated potent growth-inhibitory activities ($IC_{50} < 10$ μM) against an array of human cancer cell lines (Table 7). This group includes vobatensines A-E (**50**, **51**, **26**, **52** and **53**, respectively) and the bisindoles **54**–**57** (Fig. 9), which were isolated from an ethanolic stem bark extract. The cell line with higher sensitivity for these compounds was HT-29, with IC_{50} values ranging from 0.92 to 7.2 μM. Nevertheless, none of the compounds displayed the ability to restore the sensitivity of vincristine-resistant KB cells to vincristine (Sim et al. 2016).

Conofolidine (**58**) and conophyllidine (**59**) (Fig. 9) were also isolated from ground leaf and steam bark ethanolic extract. Both of these compounds are aspidosperma dimers and belong to the bioactive conophylline group of bisindole alkaloids (Zhang et al. 2018a). While the structural elucidation of compound **58** was reported for the first time, conophyllidine (**59**) is known since 1993 (Kam et al. 1993). Remarkably, both conofolidine (**58**) and conophyllidine (**59**) showed pronounced growth inhibitory activities ($IC_{50} \leq 1.5$ μM, Table 7) against human oral epidermoid carcinoma (KB/S), prostate carcinoma (PC-3 and LNCaP), breast adenocarcinoma (MDA-MB-231) and colorectal carcinoma (HT-29 and HCT 116) cancer cell lines (Nge et al. 2016). Furthermore, the growth inhibitory properties of conophyllidine (**59**) were later reinforced by other study, in which this compound showed potent cytotoxic activities, after a 48-h treatment against hepatic (Hep-G2, IC_{50} 0.8 μM), lung (A540, IC_{50} 1.15 μM) and gastric (SGC7901, IC_{50} 0.87 μM) cancer cell lines. In addition, this compound apparently does not interact with tubulin or microtubules. Instead, it exhibited a robust inhibitory effect on the o Nf- kB signal pathway with an IC_{50} of 0.08 μM (Zhang et al. 2018a).

Tabercorymines A (**60**) and B (**61**) (Fig. 10) containing ibogan and vobasinyl units, represent a novel class of bisindole alkaloids that were isolated from the twigs and leaves of *T. corymbosa.* Compound **60** is of particular interest due to its unique heteropentacyclic ring system, resulting from the distinctive formation a C-7/C-20 bond in the vobasinyl unit. Both compounds showed moderate activity towards various human cancer cell lines. Compound **60** displayed a slightly higher activity profile (IC_{50} ranging from 4.8 to 12.9 μM) compared to **61** (IC_{50} ranging from 9.6 to 27.9 μM). However, it is worth noting that the dehydration of **60,** leading to the formation of the C3-C14 unsaturated derivative, completely abolished its biological activity. This observation strongly suggested that the presence of the hydroxylated stereocenter at C-3 (vobasyl unit) plays a pivotal role in contributing to the antiproliferative activity of these alkaloids. Preliminary studies into the mechanism of action of compound **60**, particularly in the context of MDA-MB-231 triple-negative breast cancer cells, showed that this compound induced cell cycle arrest at G2/M phase. Notably, unlike jerantinines A (**6**), B (**39**), and E (**41**), compound **60** did not appear to interfere with microtubule formation (Yuan et al. 2017).

The vobasinyl-ibogan-type bisindole alkaloids taburnaemines A–I (**62**–**70**), isolated from the twigs and leaves, have demonstrated significant antiproliferative activities, with exception of taburnaemine B (**63**). These activities were observed across various human cancer cell lines, including the P-glycoprotein-overexpressing multidrug-resistant KB cells. The IC_{50} values for these alkaloids ranged from 2.6 to 9.8 μM (Table 7). Alkaloids **62**–**67** are characterized by the presence of 1,3-oxazinane and 1,3-oxazolidine moieties in the vobasinyl and iboga units, respectively. However, the key structural determinant influencing the antiproliferative effects of these alkaloids appeared to be the absolute configuration of the 19,20-oxirane ring (Fig. 10). This conclusion was evident when comparing the activities of taburnaemine A (**62**) and taburnaemine B (**63**) (Table 7 and Fig. 10). The beta position of the 19,20-oxirane appeared to be an essential factor for the activity, as observed not only in taburnaemine A (**62**), C (**64**) and D (**65**), but also in tabercorymine B (**61**) (Zhang et al. 2018b).

Given the notable cytotoxic activities exhibited by bisindole alkaloids when compared to monomeric units, the search for novel molecules in this class was continuously prompted. This quest led to the discovery of four new aspidosperma − aspidosperma type alkaloids, the conolodinines A − D (**71**–**74**) (Fig. 11). When tested against a vast panel of human cancer cell lines, these compounds showed pronounced in vitro growth inhibitory activities with IC_{50} values falling in the 0.01–5 μM range. However, only low activities were obtained against vincristine-resistant KB and lung cancer (A549) cells ($IC_{50} > 10$ μM). Notability, when administered along with

Table 7 Cytotoxicity of bisindole alcaloids **49–74**

Compound	Cell Line [a]/IC_{50} (μM)										Ref.
	KB/S	KB/VJ300	KB/VJ300[b]	PC-3	LNCaP	MCF-7	MDA-MB-231	A-549	HCT-116	HT-29	
Vobatensine A (**50**)	8.2	7.2	> 10	5.7	> 10	8.8	3.9	9.7	3.0	1.2	Sim et al. (2016)
Vobatensine B (**51**)	8.0	8.1	8.6	6.9	> 10	9.3	3.6	9.6	3.5	2.4	Sim et al. (2016)
Vobatensine C (**26**)	> 10	> 10	5.1	8.1	> 10	7.5	3.3	8.4	7.8	1.8	Sim et al. (2016)
Vobatensine D (**52**)	> 10	> 10	9.2	5.6	> 10	> 10	> 10	> 10	9.7	7.2	Sim et al. (2016)
Vobatensine E (**53**)	> 10	> 10	9.6	7.7	> 10	> 10	4.6	> 10	7.4	1.9	Sim et al. (2016)
16′-decarbomethoxyvoacamine (**54**)	5.3	5.0	7.0	2.8	> 10	6.0	2.5	6.8	1.6	0.93	Sim et al. (2016)
16′-decarbomethoxy dihydrovoacamine (**55**)	8.0	8.3	9.3	3.5	> 10	3.4	2.8	> 10	2.9	0.92	Sim et al. (2016)
16′-decarbomethoxyvoacamine pseudoindoxyl (**56**)	8.3	9.1	3.3	8.8	10.0	9.4	7.7	9.1	7.1	2.9	Sim et al. (2016)
Vobatricine (**57**)	> 10	> 10	> 10	5.4	> 10	8.6	4.5	9.2	6.7	1.3	Sim et al. (2016)
Conofolidine (**58**)	0.5	7.4	–	1.1	0.3	5.9	0.8	> 10	0.4	0.3	Nge et al. (2016)
Conophyllidine (**59**)	1.5	> 10	–	0.2	0.9	0.6	0.9	10.0	0.8	1.1	Nge et al. (2016)
Tabercorymines A (**60**)	9.8[c]	8.9[c]	–	–	–	12.9[c]	6.4[c]	4.8[c]	–	–	Yuan et al. (2017)
Tabercorymines B (**61**)	16.7[c]	9.6[c]	–	–	–	23.5[c]	20.5[c]	27.9[c]	–	–	Yuan et al. (2017)
Taburnaemine A (**62**)	7.4[c]	6.6[c]	–	–	–	> 10[c]	7.7[c]	8.6[c]	–	–	Zhang et al. (2018b)
Taburnaemine B (**63**)	> 10[c]	> 10[c]	–	–	–	> 10[c]	> 10[c]	> 10[c]	–	–	Zhang et al. (2018b)
Taburnaemine C (**64**)	5.7[c]	5.8[c]	–	–	–	8.3[c]	8.2[c]	5.9[c]	–	–	Zhang et al. (2018b)
Taburnaemine D (**65**)	4.7[c]	4.8[c]	–	–	–	4.6[c]	4.5[c]	4.3[c]	–	–	Zhang et al. (2018b)
Taburnaemine E (**66**)	4.8[c]	4.9[c]	–	–	–	6.0[c]	5.1[c]	4.7[c]	–	–	Zhang et al. (2018b)
Taburnaemine F (**67**)	4.8[c]	4.7[c]	–	–	–	5.6[c]	4.8[c]	5.3[c]	–	–	Zhang et al. (2018b)
Taburnaemine G (**68**)	4.5[c]	4.9[c]	–	–	–	4.9[c]	4.5[c]	4.3[c]	–	–	Zhang et al. (2018b)
Taburnaemine H (**69**)	6.7[c]	8.3[c]	–	–	–	> 10[c]	5.2[c]	9.8[c]	–	–	Zhang et al. (2018b)
Taburnaemine I (**70**)	2.7[c]	2.6[c]	–	–	–	3.0[c]	2.8[c]	3.1[c]	–	–	Zhang et al. (2018b)
Conolodinine A (**71**)	1.1	> 10	4.1	4,7	> 10	4.8	3.6	> 10	4.3	2.2	Sim et al. (2019)
Conolodinine B (**72**)	0.1	> 10	1.3	7.9	9.6	0.6	1.4	> 10	1.1	0.3	Sim et al. (2019)
Conolodinine C (**73**)	0.1	8.6	1.5	0.7	> 10	0.3	0.4	> 10	0.2	0.2	Sim et al. (2019)
Conolodinine D (**74**)	0.2	> 10	> 10	> 10	2.6	3.5	5.4	> 10	3.1	2.3	Sim et al. (2019)
Cisplatin	–	–	–	2.0	8.0	2.3	3.3	3.3	> 10	> 10	Sim et al. (2016)
Vincristine	0.002	6.6	–	–	–	0.0072	0.0326	0.0205	–	–	Sim et al. (2016)Yuan et al. (2017)

Table 7 continued

Compound	Cell Line [a]/IC_{50} (μM)										Ref.
	KB/S	KB/VJ300	KB/VJ300[b]	PC-3	LNCaP	MCF-7	MDA-MB-231	A-549	HCT-116	HT-29	
Verapamil	> 10	> 10	4.6	–	–	–	–	–	–	–	Sim et al. (2016)

[a]KB/S: vincristine-sensitive KB carcinoma. KB/VJ300: vincristine-resistant KB carcinoma. PC-3 and LNCaP: human prostate carcinoma. MCF7 and MDA-MB-231: human breast adenocarcinoma. A549: human lung carcinoma. HCT 116 and HT-29: human colorectal carcinoma. The different cell lines were treated with crescent concentrations of each compound for 72 h. IC_{50} values were determined using the MTT method. IC_{50} is the concentration of compound that inhibits 50% of cell growth. [b]With added vincristine, 0.12 μM, which did not affect the growth of the KB/VJ300 cells. [c]IC_{50} values were determined using the SRB method

vincristine, conolodinines A − D (**71**–**74**) proved to be able to restore the sensitivity of KB/VJ300 cells to the anticancer drug (Table 7) (Sim et al. 2019).

The aspidosperma-aspidosperma taberyuine A – C (**75**–**77**), and the ivobasinyl-ibogan bisindoles taberyuines H (**78**) and I (**79**) (Fig. 12) were also tested for their antiproliferative activities. Taberyuines A (**75**) and C (**77**), H (**78**) and I (**79**) showed only moderated activity, with IC_{50} values ranging between 2.4 and 16.8 μM, when assessed in human liver (HepG2), lung (A549) and gastric (SGC7901) cancer cell lines after 48-h exposure (Table 8). In contrast, taberyuine B (**76**) presented stronger cytotoxic properties, with IC_{50} values raging between 0.7 and 2.1 μM. According to these results, it became evident that the 14′,15′-epoxy moiety has a detrimental effect on cytotoxic activity. Conversely, the presence of the furan ring in structures **75**–**77** appeared to be crucial for activity, as several other taberyuines (D, E, F, and G), lacking this moiety, exhibited no activity against the tested cell lines. The transcription factor NF-κB lays a pivotal role in the regulation of immune and inflammatory responses, which are frequently involved in pathogenesis and treatment of cancers. Preliminary studies suggested that the mode of action of taberyuine B (**76**) involves the inhibition of the NF-kB signal pathway (IC_{50} 0.18 μM) (Zhang et al. 2018a).

It is well-established that targeting autophagy in cancer treatment holds promise as a therapeutic strategy, but it also represents a double-edge sword effect. On one hand, autophagy suppresses tumourigenesis by limiting the production of reactive oxygen species and DNA damage. However, it subsequently adapts to support the survival of cancer cells and fosters the tumourigenicity of cancer stem cells at established sites. Consequently, the intricate autophagic process, governed by an array of proteins, emerges as an appealing target for cancer therapy. Thus, the use of autophagy modulators as adjuvant therapy has been explored by researchers (Lim et al. 2021). In this context, Xiao-Jiang Hao explored the potential of a series of monoterpenoid indole alkaloids sourced from *T. corymbosa* to modulate autophagy. Compounds such as taberine D (**80**), tabernaelegantine B (**81**), conodurine (**82**) and tabernaricatine C (**83**) (Fig. 13) demonstrated the ability to disrupt the autophagic flux. This effect appears to be associated with the attenuation of lysosomal acidification, thereby impeding the fusion of autophagosomes and lysosomes. In addition,

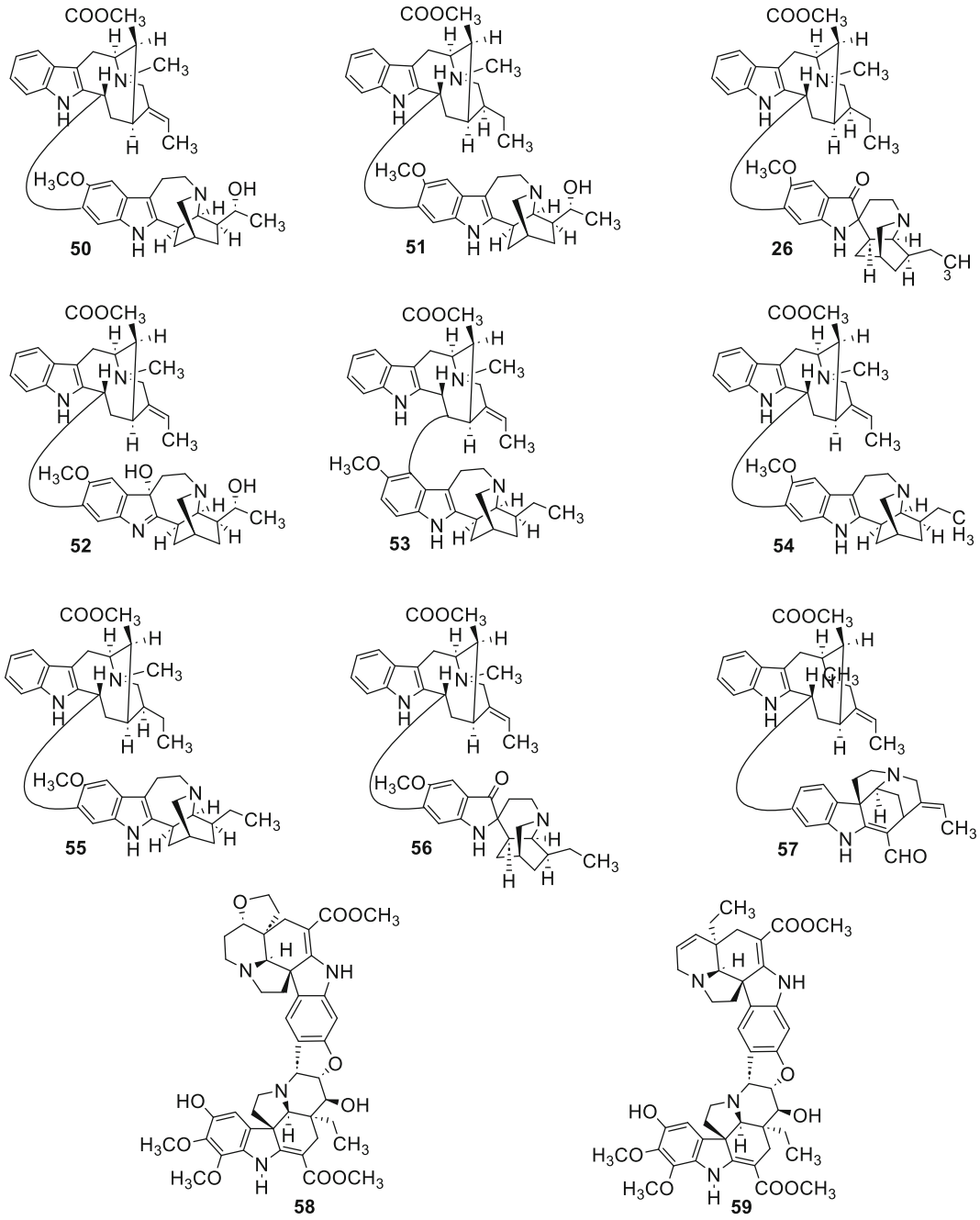


Fig. 9 Chemical structures of bisindole alkaloids vobatensine A-E (**50, 51, 26, 52, 53**); decarbomethoxyvoacamine (**54**), dihydrovoacamine (**55**), 16′-decarbomethoxyvoacamine pseudoindoxyl (**56**), vobatricine (**57**), conofolidine (**58**) and conophyllidine (**59**)

compounds **80** and **83** also exhibited cytotoxic potency on par with that of cisplatin across various human cancer cell lines. These cumulative observations unveil new molecular mechanism underlying anti-cancer effects of these indole alkaloid compounds (Zhang et al. 2020).

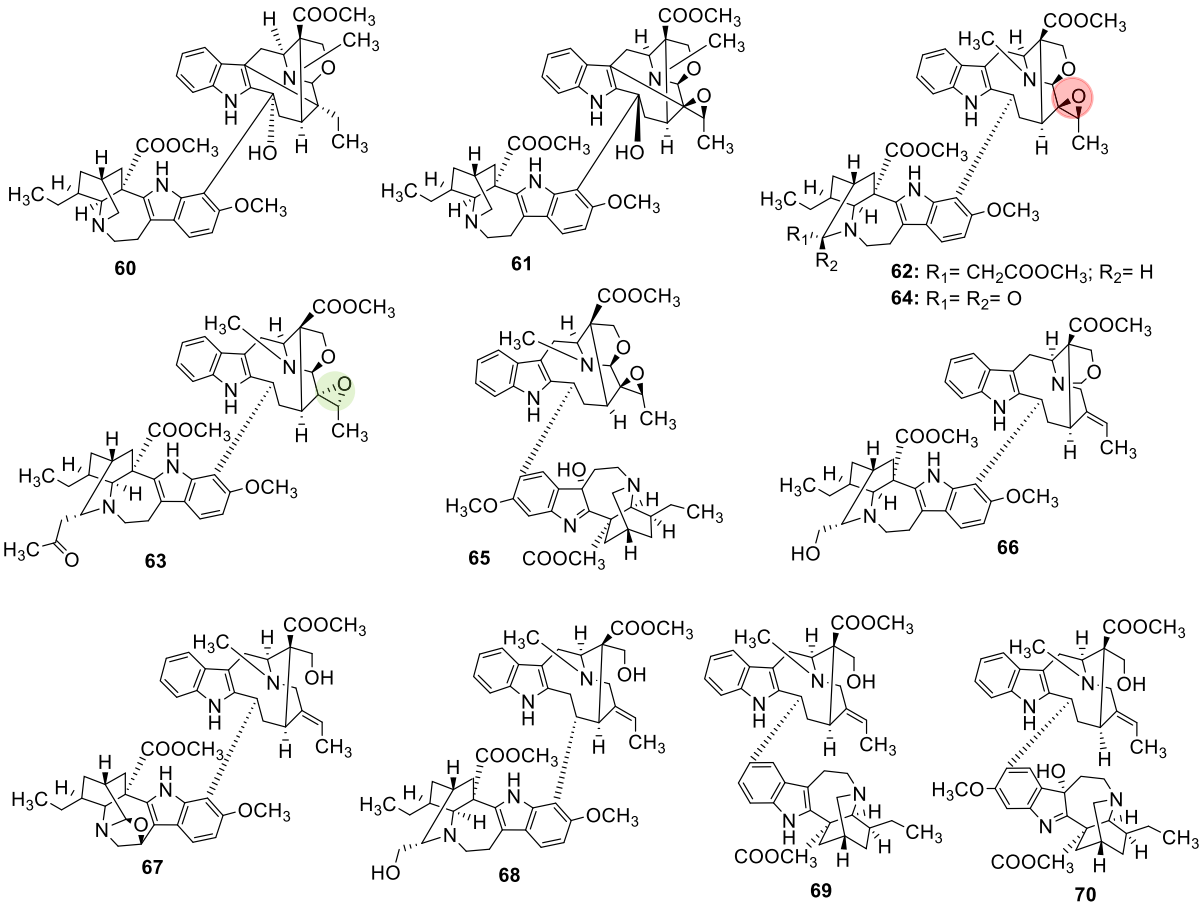


Fig.10 Chemical structures of tabercorymines A (**60**) and B (**61**) and taburnaemines A–I (**62–70**). The configuration of the 19,20-oxirane ring of compounds **62** and **63** is highlighted in red and green

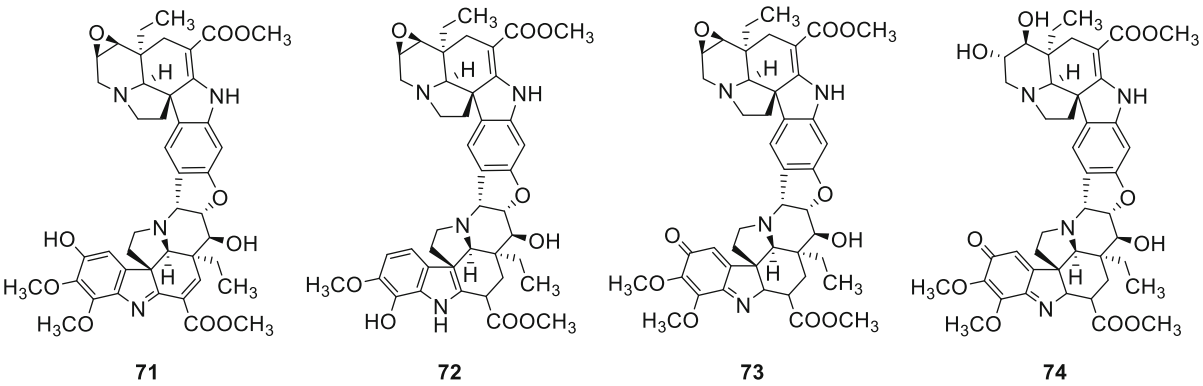


Fig.11 Chemical structures of conolodinines A–D (**71–74**)

Tabernaemontana divaricata

T. divaricata (L.) R. Br. ex Roem. & Schult (syn. *Ervatamia divaricata*) is an evergreen shrub or small tree, commonly known as Crepe Jasmine. The species is widely distributed in Asia, Australia, mangrove forest of China, Japan and India, being also cultivated as ornamental plant due to its shiny deep green leaves

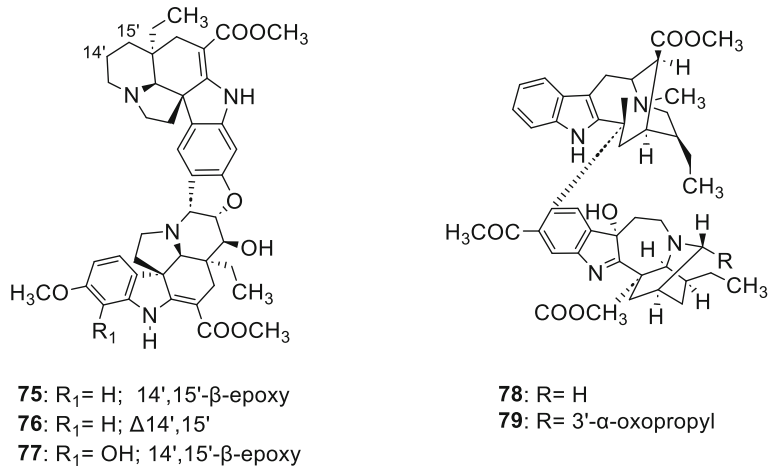


Fig. 12 Chemical structures of taberyuines A–C (**75**–**77**), H (**78**) and I (**79**)

Table 8 Cytotoxicity of taberyuines A–C (**75**–**77**), H (**78**) and I (**79**)

Compound	Cell Line/IC_{50} (μM)[a]			Ref.
	Hep-G2	A549	SGC7901	
Taberyuine A (**75**)	12.3	16.8	9.8	Zhang et al. (2018a)
Taberyuine B (**76**)	1.5	2.1	0.7	Zhang et al. (2018a)
Taberyuine C (**77**)	15.8	16.8	14.2	Zhang et al. (2018a)
Taberyuine H (**78**)	3.5	5.1	2.4	Zhang et al. (2018a)
Taberyuine I (**79**)	4.1	4.7	3.1	Zhang et al. (2018a)
Camptothecin	0.5	0.4	0.3	Zhang et al. (2018a)

[a]Hep-G2: Human liver cancer; A549: Human lung cancer; SGC7901: Human gastric cancer cell lines. The different cell lines were treated with crescent concentrations of each compound for 48 h. IC_{50} values were determined using MTT method. IC_{50} is the concentration of compound that inhibits 50% of cell growth

and white colored fragrant flowers (Ghosh et al. 2021). Various parts of *T. divaricata* have been extensively used in Ayurvedic, Chinese and Thai traditional medicines for the treatment of a several human ailments due to the antioxidant, anti-tumour, and analgesic properties. It is used to treat fever, headache, dysentery, vomiting and diarrhea, abdominal tumours, inflammation, leprosy, and asthma. Additionally, it is also used as anthelminthic, antihypertensive, and as tonic for brain, liver, and spleen (Pratchayasakul et al. 2008; Bhadane et al. 2018; Ghosh et al. 2021).

Taberdivarines A–B (**84**–**85**) were isolated from the leaves of the plant, being the first aspidosperma–aspidosperma-aspidosperma alkaloid trimers with a furan ring linkage (Chen et al. 2021). Moreover, six new dimers named taberdivarines C–H[1] (**86**–**91**) were also reported (Fig. 14). The cytotoxicity of taberdivarines A–H (**84**–**91**) was evaluated against three human cancer cell lines, SMMC-7721 (hepatocellular carcinoma), HT-29 (colorectal adenocarcinoma) and A549 (non-small cell lung) by the MTS assay (Table 9). Taberdivarine F (**89**) was the most cytotoxic compound against the three cell lines, displaying IC_{50} values of 0.30 (SMMC-7721), 0.75 (HT-29) and 3.41 (A549) μM, comparable to those obtained for the positive control vinolrebine (IC_{50} values of 3.02, 0.14 and 2.23 μM, respectively). Compounds **90** and **91** were also very active against SMMC-7721 cells (IC_{50} values of 1.72 and 2.01 μM), and HT-29 and A549 carcinoma cells (IC_{50} values ranging from 4.05 to 9.73 μM). Similar IC_{50} values were obtained for taberdivarine A (**84**) on all cell lines tested, while taberdivarines C (**86**) and D (**87**) showed a moderate

[1] This name is used by other authors to name compounds with different structures.

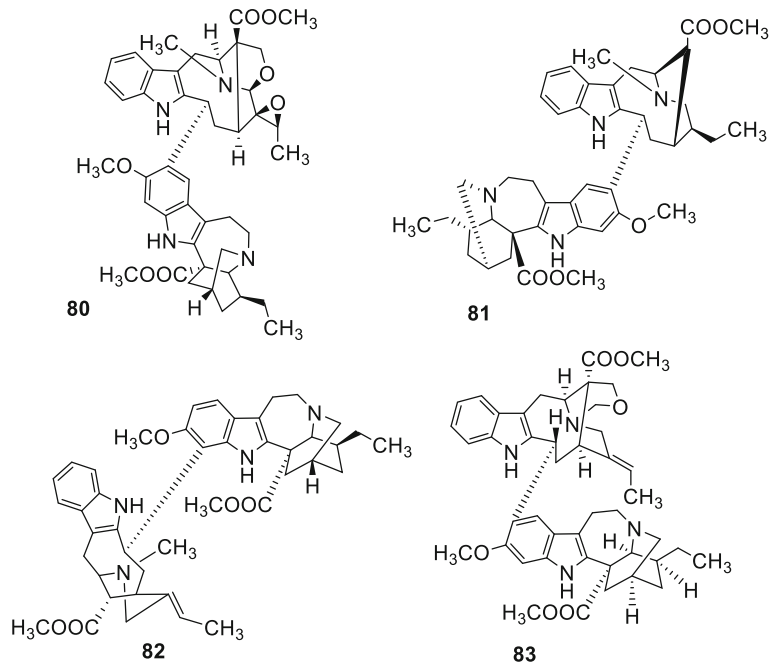


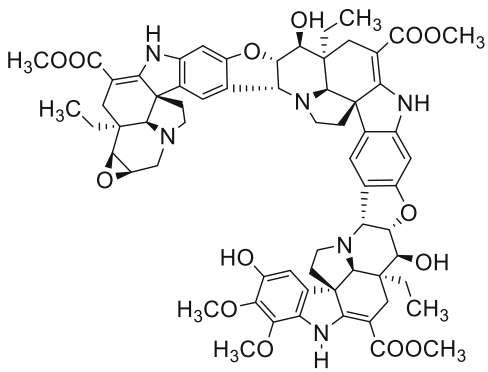
Fig. 13 Chemical structures of taberine D (**80**), tabernaelegantine B (**81**), conodurine (**82**) and tabernaricatine C (**83**)

cytotoxic activity against SMMC-7721 and HT-29 cancer cells but were non cytotoxic on A549 cell line ($IC_{50} > 40$ μM). Compounds **85** and **88** showed no cytotoxicity (Chen et al. 2021).

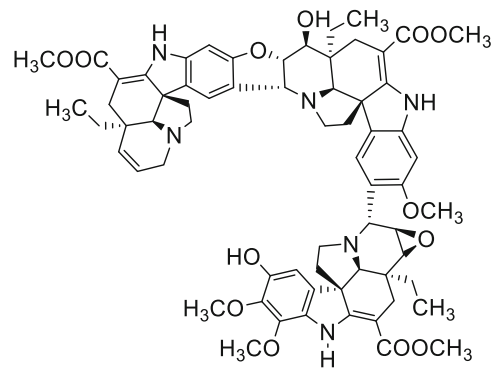
Zhang et al. isolated five new vobasinyl−ibogan-type bisindole alkaloids, tabernaricatines A−E (**83, 92–95**), and two new monomers, tabernaricatines F and G (**96** and **97**) from the aerial parts of *T. divaricata* (Fig. 15) (Zhang et al. 2013). Several known indole alkaloids, including ervachinine A–C (**98–100**), cononitarine B (**101**), conofoline (**102**) (Fig. 16) and conophylline (**24**) (Fig. 5) were also isolated. Tabernaricatines A (**92**) and B (**93**) were the first examples of alkaloids possessing a vobasine–iboga scaffold with a six-membered ring formed by an ether linkage between C-17 and C-21 in the vobasine unit. Excepting for compound **83**, all the isolated alkaloids were assayed for their cytotoxicity against five human cancer cell lines (HL-60, SMMC-7721, A-549, MCF-7 and SW480). Compounds **93** and **94–96** were found to be non-cytotoxic ($IC_{50} > 40$ μM). Among the cytotoxic compounds it was interesting to observe a higher activity against the human myeloid leukaemia (HL-60) cell line (IC_{50} 0.17–3.88 μM) when comparing with the other cancer cell lines (Table 9). Particularly, conophylline (**24**) showed the strongest activity against all the cell lines tested, (IC_{50} values ranging from 0.17 to 1.49 μM), being even more cytotoxic than cisplatin (IC_{50} between 1.14 and 16.84 μM), used as positive control. Tabernaricatine A (**92**) also exhibited significant inhibitory effects on HL-60 (0.79 μM), SMMC-7721 (3.41 μM), A-549 (3.52 μM), MCF-7 (3.10 μM), and SW480 (2.59 μM). Tabernaricatine G (97), ervachinines A-C (**98–100**), and conofoline (**102**) displayed moderate cytotoxicity against A-549, MCF-7 and SW480 cell lines (IC_{50} 10.35–28.53 μM) (Zhang et al. 2013).

From the stems of the plant, several alkaloids were isolated, including the new monoterpenoid bisindole compounds flabellipparicine (**103**), 19,20-dihydrovobparicine[2] (**104**), 10′- demethoxy-19,20-dihydrovobatensine D (**105**), and 3′-(2-oxopropyl)ervahanine A (**106**). Deoxytubulosine (**112**), a β-carbolinebenzoquinolizidine alkaloid was also obtained (Fig. 17) (Cai et al. 2018). Flabellipparicine (**103**) features an uncommon flabelliformide-apparicine-type scaffold linked with a C-3 − C-22′, and a N-1 − C-16′ bonds giving rise to the five-membered ring between the two monomers. All compounds were screened for their cytotoxic activity against human breast (MCF-7) and human lung (A-

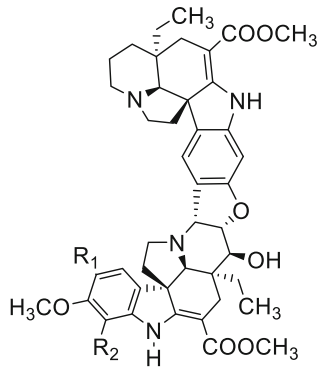
[2] This name is also used to name other compound with a different structure.

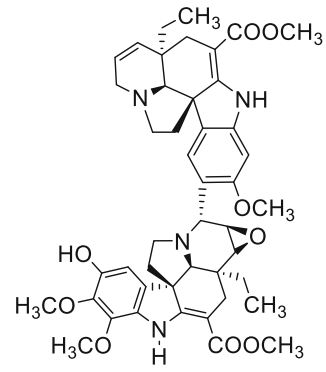


84



85





91

86: R_1= OH; R_2= OCH_3 14',15'-α-epoxy
87: R_1= OH; R_2= OCH_3 14',15'-β-epoxy N_4-oxide
88: R_1= OH; R_2= H 14',15'-β-epoxy
89: R_1= H; R_2= OCH_3 $\Delta^{14',15'}$
90: R_1= H; R_2= OH $\Delta_{14',15}$

Fig. 14 Chemical structures of taberdivarines A–H (**84**–**91**)

549) cancer cell lines, using 7-ethyl-10-hydroxy-camptothecin (SN38) as positive control (IC_{50} values of 0.1 and 0.2 nM, respectively) (Table 10). Deoxy-tubulosine (**112**) was significantly cytotoxic displaying IC_{50} values of 2 and 90 nM, respectively. Among the bisindole alkaloids set, the most active compounds were those possessing two indole NH groups (**104**, **106**–**109** and **4**), which showed IC_{50} values ranging from 0.8 μM (**104**) to 7.3 (**108**) μM on MCF-7 cell line, 1.2 μM (**106**) and 8.1 μM (**104**) on A-549 cell line. On the other hand, alkaloids **103** and **105**, having only one indole NH group showed IC_{50} values higher than 10 μM on MCF-7 and A-549 cell lines, respectively (Cai et al. 2018).

Two unique vobasine-iboga-vobasine-type alkaloids, ervadivamines A (**113**) and B (**114**) were also isolated from the roots ethanolic extract (Liu et al. 2018). These trimers were the first alkaloids containing two different types of constitutional units, linked through C-3−C-11′ and N-1′−C-3″ bonds, respectively (Fig. 18). Interestingly, the dimeric (19,20-dihydroervahanine A, **115**) and monomeric (bogamine and ibogaine) precursors were also isolated, which allowed the proposal of a biogenetic pathway. Compound **115** exhibited significant cytotoxic activity against HT-29 (IC_{50} 3.44 μM) and A549 (IC_{50} 8.74 μM), displaying higher IC_{50} values against MCF-7 and HepG2/ADM (hepatocellular carcinoma adriamycin-selected multidrug resistant) cell lines

Table 9 Cytotoxicity of compounds **84–102**

Compound	Cell Line/IC_{50} (μM)[a]						Ref.
	MCF-7	A549	HT-29	HL-60	SMMC-7721	SW480	
Taberdivarine A (**84**)	–	10.44	11.41	–	4.96	–	Chen et al. (2021)
Taberdivarine B (**85**)	–	> 40	> 40	–	> 40	–	Chen et al. (2021)
Taberdivarine C (**86**)	–	> 40	36.02	–	20.12	–	Chen et al. (2021)
Taberdivarine D (**87**)	–	> 40	19.87	–	13.02	–	Chen et al. (2021)
Taberdivarine E (**88**)	–	> 40	> 40	–	> 40	–	Chen et al. (2021)
Taberdivarine F (**89**)	–	0.75	0.75	–	0.30	–	Chen et al. (2021)
Taberdivarine G (**90**)	–	5.96	4.05	–	1.72	–	Chen et al. (2021)
Taberdivarine H (**91**)	–	9.73	5.89	–	2.01	–	Chen et al. (2021)
Tabernaricatine A (**92**)	3.10	352	–	0.79	3.41	2.59	Zhang et al. (2013)
Tabernaricatine G (**97**)	13.23	28.53	–	3.88	14.75	13.01	Zhang et al. (2013)
Ervachinine A (**98**)	13.26	16.51	–	2.35	9.86	16.54	Zhang et al. (2013)
Ervachinine B (**99**)	13.23	28.53	–	3.88	14.75	13.01	Zhang et al. (2013)
Ervachinine C (**100**)	12.61	14.75	–	2.68	12.35	13.43	Zhang et al. (2013)
Cononitarine B (**101**)	3.02	9.40	–	2.90	3.75	2.72	Zhang et al. (2013)
Conofoline (**102**)	14.00	10.35	–	0.80	10.35	13.67	Zhang et al. (2013)
Conophylline (**24**)	1.02	0.21	–	0.17	0.35	1.49	Zhang et al. (2013)
Vinolrebine	–	2.23	014	–	3.02	–	Chen et al. (2021)
Cisplatin	17.18	12.76	–	1.14	14.51	16.84	Zhang et al. (2013)

[a]MCF-7 (human breast adenocarcinoma), A549 (non-small cell lung), HT-29 (colorectal adenocarcinoma), HL-60 (human myeloid leukaemia), SMMC-7721 (hepatocellular carcinoma), and SW480 (colon cancer); IC_{50} values were determined by MTT assay, following 48 h exposure of cells to test agents. IC_{50} is the concentration of compound that inhibits 50% of cell growth

(19.49 and 16.63 μM, respectively). Among the new isolated trimers, ervadivamine A (**113**) was cytotoxic against all cancer cell lines (IC_{50} ranging from 10.25 to 12.55 μM), including the adriamycin-resistant HepG2 cell line. Curiously, ervadivamine B (**114**) that differs from ervadivamine A (**113**) by having an additional methoxy group at C-10′ (ibogain moiety) was inactive against the MCF-7 and HepG2/ADM cell lines ($IC_{50} > 50$ μM) (Liu et al. 2018).

Lirofolines A (**35**) and B (**116**) are pentacyclic indole alkaloids having a new rearranged ibogan ring, isolated from *T. corymbosa* and *T. divaricata*, respectively (Low et al. 2010). Despite being non-cytotoxic against both drug-sensitive and vincristine-resistant KB cells, both alkaloids demonstrated multidrug resistance reversing effect in vincristine-resistant KB cells with IC_{50} of 10.5 and 21.2 μM, respectively, in the presence of 0.12 μM of vincristine (Low et al. 2010).

Tabernaemontana elegans

T. elegans Stapf. is a shrub or small tree found in East and Southeastern Africa, including Mozambique. It is used in African traditional medicine for treating several diseases. The powdered root bark or fruits have been used to treat cancer. Decoction of root has been used for washing wounds and to treat pulmonary diseases, while maceration of root ash is drunk to treat tuberculosis. The use of roots, stem bark and seeds for treating heart diseases is also reported (PROTA Foundation 2008).

Aiming at obtaining new plant-derived anticancer compounds with emphasis on targeting multidrug resistance in cancer, our research group has been carrying out the phytochemical study of the alkaloid fractions of the methanol extracts of leaves and roots of *T. elegans,* which allowed the isolation of several indole alkaloids, including *β*-carbolines, and monoterpene indole alkaloids of the corynanthe-type. Several bisindole alkaloids of the vobasinyl-iboga-type were also isolated (Ferreira and Paterna 2019). As reviewed,

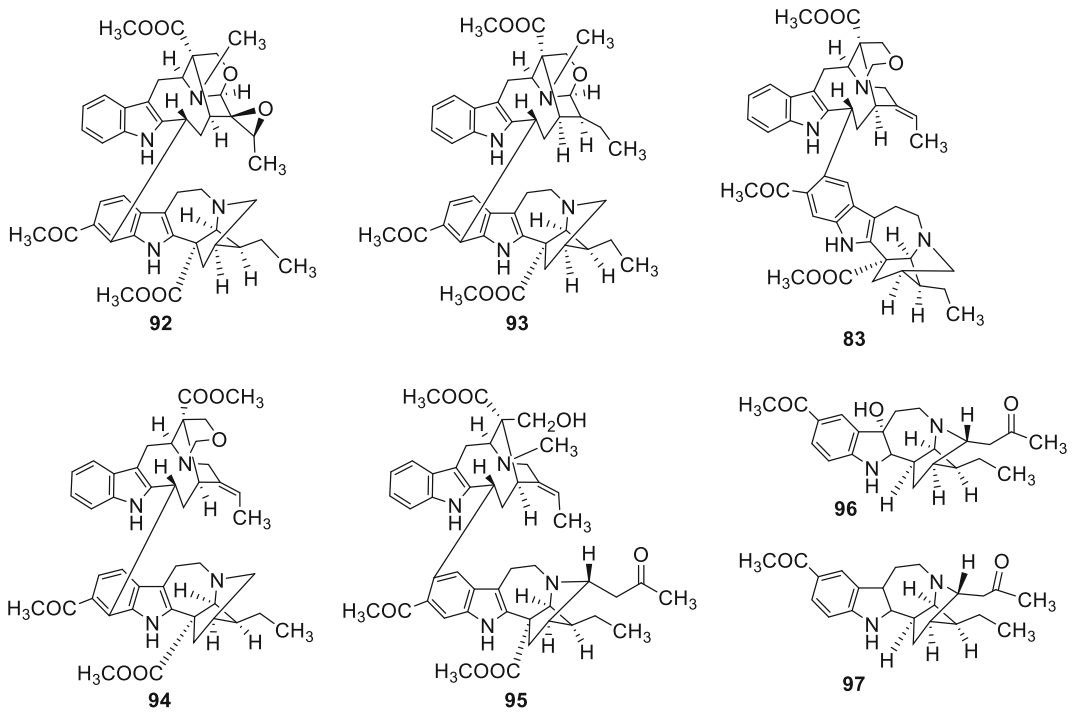
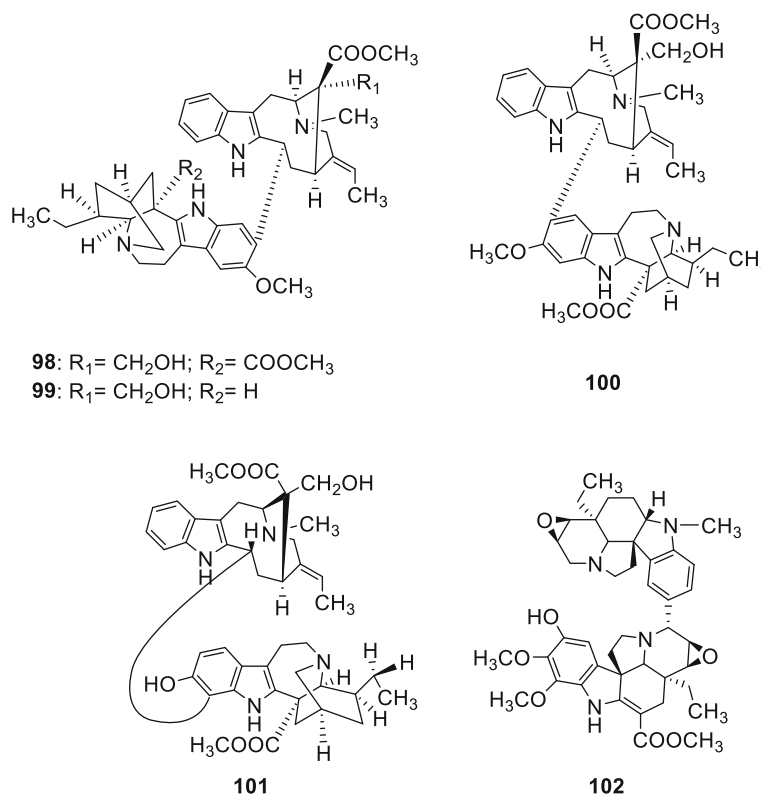


Fig. 15 Chemical structures of bisindole alkaloids tabernaricatines A–E (**83, 92–95**) and the monomers tabernaricatines F (**96**) and G (**97**)

Fig. 16 Chemical structures of indole alkaloids **98–102** isolated from *T. divaricata*



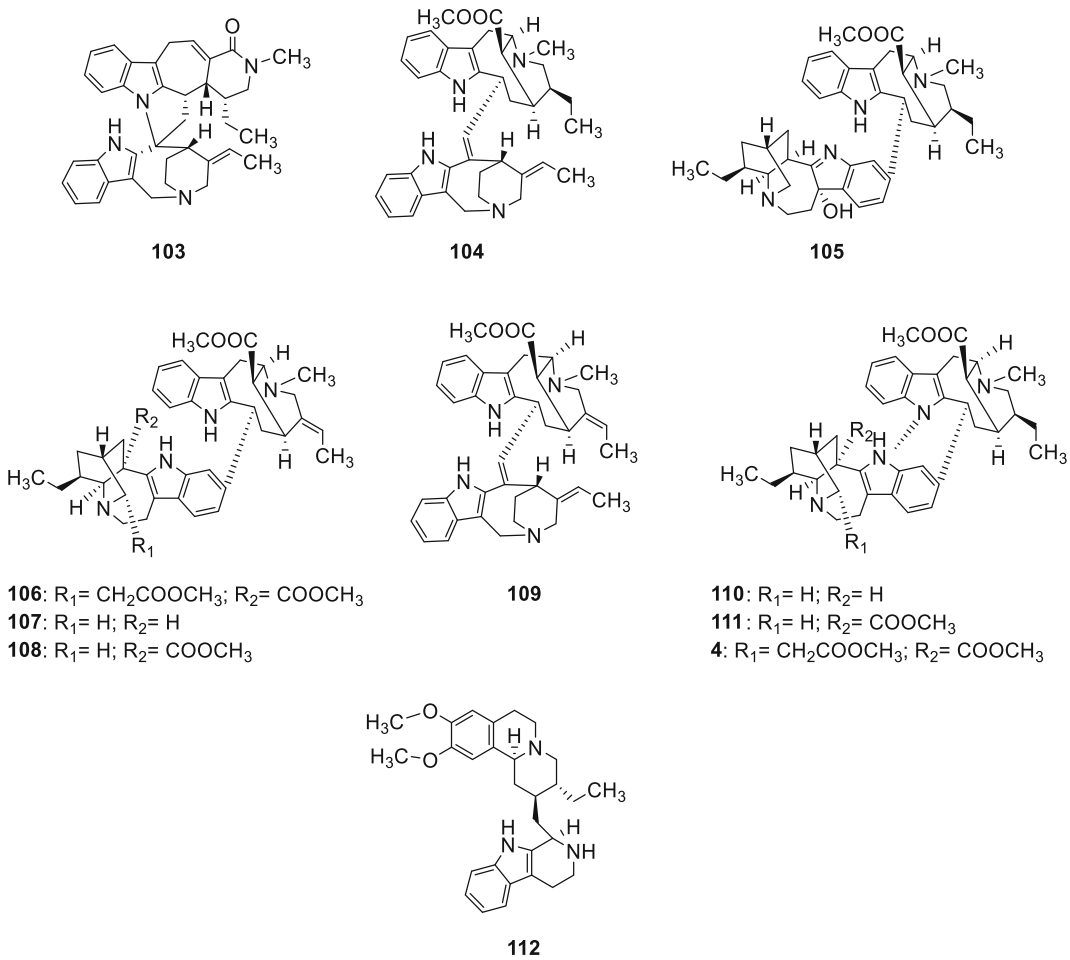


Fig. 17 Chemical Structures of bisindole alkaloids (**4**, **103**–**112**) isolated from *T. divaricata*

aiming at generating a library of new compounds sharing the monoterpene indole alkaloid scaffold, tabernaemontanine (**117**) and dregamine (**118**), two major epimers found in *T. elegans* with a monoterpene indole alkaloid scaffold of the corynanthe-type, were derivatized through condensation of the ketone group with different amine derivatives, to yield several compounds with new nitrogen-containing aromatic and aliphatic moieties. Condensation of tabernaemontanine (**117**) and dregamine (**118**) with hydrazine hydrate and further reaction with different aldehydes yielded azines. Acyl derivatives were also prepared after reduction of compounds **117** and **118** (Fig. 19) (Ferreira and Paterna 2019).

As detailed previously (Ferreira and Paterna 2019), some of the referred natural indole and bisindole alkaloids were able to induce apoptosis and to arrest cell cycle, whereas the derivatives were found to be P-gp and MRP1 inhibitors in resistant cancer cells, overexpressing these ABC transporters. Compounds with selective toxicity against resistant cancer cells overexpressing MRP1 were also reported. It was concluded that the introduction of aromatic nitrogen-containing moieties at the carbonyl group of the indole alkaloid scaffold of tabernaemontanine (**117**) and dregamine (**118**) increased significantly the capacity of some compounds as P-gp inhibitors when compared with the starting natural compounds (Ferreira and Paterna 2019).

Consequently, based on the previous encouraging results and aiming at increasing the number of analogous for structure–activity relationship studies, a new set of *N*-alkylated derivatives was prepared through reaction of the indole nitrogen of compounds

Table 10 Cytotoxicity of compounds **103–115**

Compound	Cell Line/IC_{50} (μM)[a]			Ref.
	MCF-7	A549	HT-29	
Flabellipparicine (**103**)	> 10	7.5	–	Cai et al. (2018)
19,20-dihydrovobparicine (**104**)	0.8	8.1	–	Cai et al. (2018)
10′- demethoxy-19,20-dihydrovobatensine D (**105**)	1.3	> 10	–	Cai et al. (2018)
3′-(2-oxopropyl)ervahanine A (**106**)	2.8	1.2	–	Cai et al. (2018)
Tabernamine (**107**)	1.3	3.2	–	Cai et al. (2018)
Ervahanine A (**108**)	7.3	1.2	–	Cai et al. (2018)
9,10-vobparicine (**109**)	1.3	4.0	–	Cai et al. (2018)
19,20-dihydrotabernamine A (**111**)	5.4	> 10	–	Cai et al. (2018)
Deoxytubulosine (**112**)	0.002	0.09	–	Cai et al. (2018)
Ervadivamine A (**113**)	11.27	10.25	11.37	Liu et al. (2018)
Ervadivamine B (**114**)	> 50	31.73	15.78	Liu et al. (2018)
19,20-dihydroervahanine A (**115**)	19.49	8.74	3.44	Liu et al. (2018)
SN38	< 0.1 nM	0.2	–	Cai et al. (2018)
Adriamycin	1.51	0.97	1.48	Liu et al. (2018)

[a]MCF-7 (human breast adenocarcinoma), A549, and HT-29 (colorectal adenocarcinoma). IC_{50} values were determined by SRB assay, following 72 h exposure of cells to test agents; IC_{50} values of ervadivamines A-B, 19,20-dihydroervahanine A, and adriamycin were determined by the MTT assay, following 72 h exposure of cells to test agents. IC_{50} is the concentration of compound that inhibits 50% of cell growth

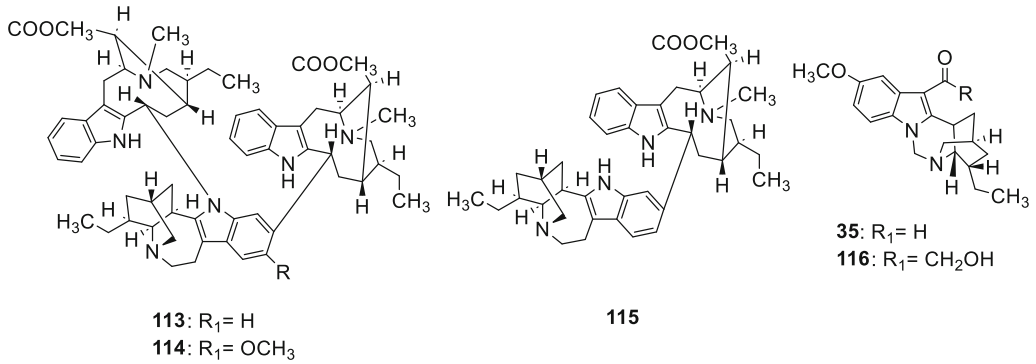


Fig. 18 Chemical structures of bisindol alkaloids **113–115** and lirofolines A (**35**) and B (**116**) isolated from *T. divaricata*

117 and **118**, with different aliphatic and aromatic halides, yielding twenty-six new *N*-alkylated derivatives (Fig. 19) (Cardoso et al. 2021a).

Likewise, and aiming mostly to obtain new derivatives containing new nitrogen atoms and aromatic rings, two new set of compounds were also prepared by condensation of the carbonyl at C-3 of dregamine (**118**) with hydrazine followed by reaction with different aldehydes, to obtain nineteen new azines (**145–163**) (Fig. 20), whereas the reaction of with isocyanates yielded eleven new semicarbazones (**164–174**) (Fig. 21)(Cardoso et al. 2021b).

MDR reversal activity

All *N*-alkylated (**119–144**), azine (**145–163**) and semicarbazone (**164–174**) derivatives were evaluated for their MDR reversal ability, by functional and chemosensitivity assays, using as model resistant human *ABCB1*-gene transfected L5178Y mouse

lymphoma cells, overexpressing P-glycoprotein. In the functional assay, the capability of compounds was measured by determining fluorescence activity ratio (FAR) values, measuring the cytoplasmic accumulation of rhodamine-123, by flow cytometry. Verapamil, a known P-gp inhibitor, was used as positive control (Cardoso et al. 2021a, b).

When comparing with the starting compounds, which were practically inactive (**117** and **118**), an important increase of activity was found for most of the derivatives. In the set of *N*-alkylated derivatives (**119–144**), which were not cytotoxic or showed weak cytotoxicity, the most active compounds in the transport assay, were those sharing *N*-phenethyl moieties (**141–144**), with bromo or methoxy substituents, displaying remarkable P-gp inhibitory activity. At the lowest concentration (2 μM), compound **143**, which was not cytotoxic, was the strongest P-gp inhibitor (Table 11), exhibiting more than 20-fold higher activity than the positive control, verapamil, at 20 μM. Strong activity was also found for compounds containing a *N*-benzyl substituted with a halogen atom (**125–128** and **134**) (Table 11). Most of dregamine derivatives were stronger P-gp inhibitors than the corresponding derivatives of tabernaemontanine (**117**) suggesting that the stereochemistry at C-20 might be import for the activity. The MDR reversal activity of this set of derivatives was corroborated in chemosensitivity assays, exhibiting most of the derivatives tested very strong synergism with doxorubicin (combination index, CI < 0.1), being the most effective compounds **143** and **144**.

In QSAR models, which were generated for having further insights on the structural features important for effective drug-receptor interactions, it was concluded that compounds bearing bulky and lipophilic substituents were stronger P-gp inhibitors.

Similarly, significant MDR reversal activity was observed for dregamine azine (**145–163**) and semicarbazone (**134–174**) derivatives (Figs. 20 and 21). When comparing the antiproliferative activity with that of the starting compound **118** (IC_{50} 37.21 μM, sensitive cells; 22.97 μM, resistant cells), conversely to *N*-alkylated analogous, most of the derivatives showed higher antiproliferative activity against both sensitive L5178Y mouse T-lymphoma cells (PAR) and resistant human *ABCB1*-gene transfected L5178Y subline (MDR) (IC_{50} values ranging from 5.43 to 26.40 μM, sensitive cells; 4.28 to 12.91 μM, resistant cells). Moreover, most of the compounds showed selectivity against the MDR cells (relative resistance, RR < 1) exhibiting compounds **147**, **149**, **151**, **153**, **155**, **156**, **165**, **166**, collateral sensitivity effect (RR ≤ 0.5). The MDR-selective properties of these compounds, in P-gp-overexpressing cells, might be explained, at least partially, by their possible metal-chelating properties (Heffeter et al. 2019) (Table 12).

When comparing with dregamine (**118**), an important increase of P-gp inhibitory activity was also observed for most of these compounds, mainly those containing an azine moiety with aromatic substituents, being compounds with trimethoxy-phenyl (**159**), or naphthyl motifs (**160** and **161**) the strongest P-gp inhibitors at the lowest concentration (0.2 μM; FAR $>$ 10; Table 13). At 2 μM, a remarkable inhibition of P-gp efflux activity was found for most of the azines with aromatic moieties, being the strongest inhibitors compounds **158–163** (FAR > 95.5). On the contrary, no significant activity was found for the azine derivative with an aliphatic moiety (**145**). Conversely to azines, the semicarbazone derivatives of dregamine (**164–174**) exhibited significant activity only at the highest concentration tested (2 μM), being more active also those compounds bearing aromatic moieties (**167–174**) (FAR values of 3.20–8.77 at 2 μM).

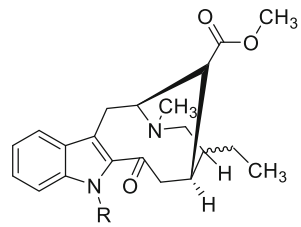
The results obtained for these derivatives corroborated the importance of the introduction of new aromatic moieties to the indole alkaloid scaffold for enhancing the activity by generating extra electrostatic and π-π interactions with the amino acid residues with P-gp. The role of H-bonding acceptor potential of P-gp inhibition was also evidenced in this study.

In drug combination assays, most of the compounds of both sets synergized doxorubicin in the same cell lines, substantiating their potential as MDR reversers. Selected azine and semicarbazone derivatives (**154**, **159**, **160**, **162** and **171**) were found to behave as inhibitors in the ATPase activity assay. Likewise in the set of *N*-alkylated derivatives, in generated QSAR models, it was deduced that lipophilicity and bulkiness features of compounds were related with higher P-gp inhibitory activity.

Homologous DNA repair inhibitors

The treatment of triple-negative breast and advanced ovarian cancer remains a great challenge, relying mostly on platinum drugs and currently on Poly (ADP-

Fig. 19 *N*-alkylated derivatives (**119–144**) of tabernaemontanine (**117**) and dregamine (**118**)

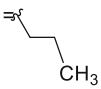


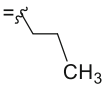
117: β-CH_2CH_3; R = **H**

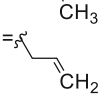
118: α-CH_2CH_3; R = **H**

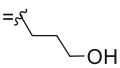
119: β-CH_2CH_3; R = 

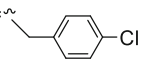
120: α-CH_2CH_3; R = 

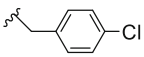
121: β-CH_2CH_3; R = 

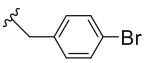
122: β-CH_2CH_3; R = 

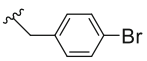
123: β-CH_2CH_3; R = 

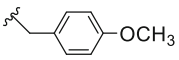
124: β-CH_2CH_3; R = 

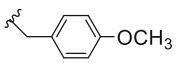
125: β-CH_2CH_3; R = 

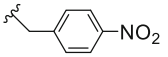
126: β-CH_2CH_3; R = 

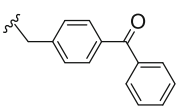
127: β-CH_2CH_3; R = 

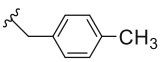
128: α-CH_2CH_3; R = 

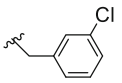
129: β-CH_2CH_3; R = 

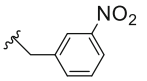
130: β-CH_2CH_3; R = 

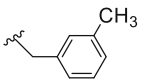
131: β-CH_2CH_3; R = 

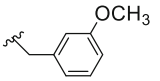
132: β-CH_2CH_3; R = 

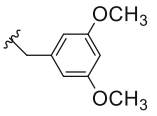
133: β-CH_2CH_3; R = 

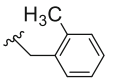
134: β-CH_2CH_3; R = 

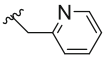
135: β-CH_2CH_3; R = 

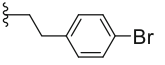
136: β-CH_2CH_3; R = 

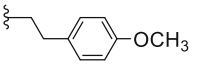
137: β-CH_2CH_3; R = 

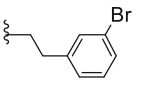
138: β-CH_2CH_3; R = 

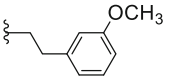
139: β-CH_2CH_3; R = 

140: β-CH_2CH_3; R = 

141: β-CH_2CH_3; R = 

142: β-CH_2CH_3; R = 

143: β-CH_2CH_3; R = 

144: β-CH_2CH_3; R = 

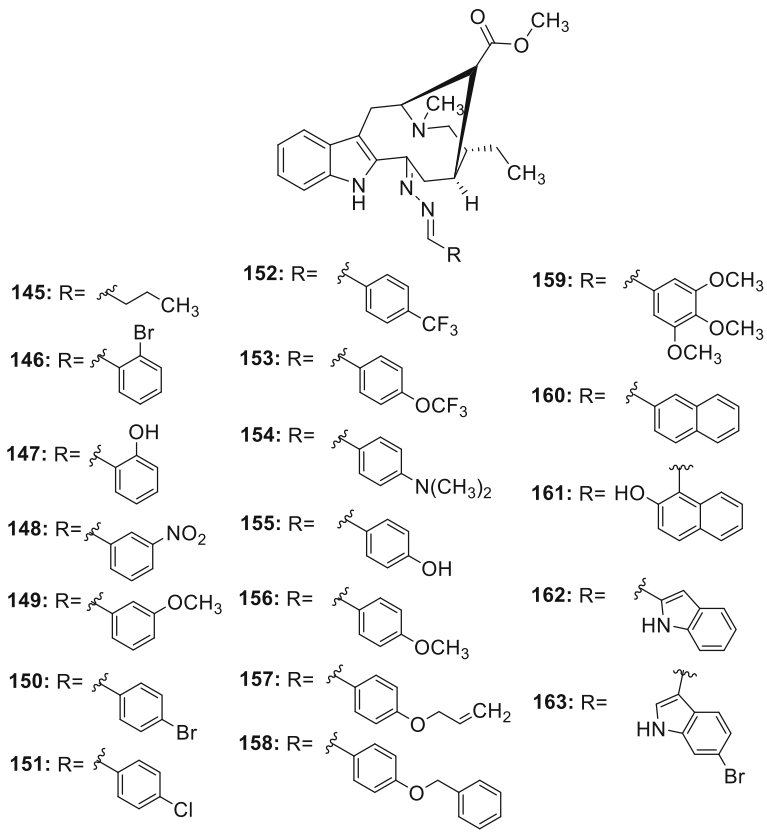


Fig. 20 Azine (**145**–**163**) dregamine derivatives

ribose) polymerase (PARP) inhibitors, such olaparib, which are in the frontline for the treating of breast and ovarian cancer with BRCA-deficient tumours. However, despite PARP inhibitors success, resistance to these agents has been reported, limiting their clinical use. Therefore, therapeutic alternatives, for sensitizing cancer cells to the effect of PARP inhibitors and other anticancer agents, are very important in cancer therapy. Recently, we have identified a dregamine hydrazone derivative (**175**, Fig. 22) that targeted homologous recombination DNA repair defects, by disrupting BRCA1-BARD1 heterodimer complex, in triple-negative breast and ovarian cancers (Raimundo et al. 2021) To evaluate its antitumour activity and molecular mechanism of action, two- and three-dimensional cell cultures with different BRCA1 status, as well as patient-derived cell lines and xenograft mice models were used.

BBIT20 (**175**) was highly effective, mostly against triple-negative breast cancer cells (IC_{50} values ranging from 4 to 6 μM in BRCA1-deficient cancer cells) when compared to cisplatin and the targeted drug olaparib, which showed much higher IC_{50} values. Moreover, BBIT20 (**175**) showed selectivity to cancer cells displaying much lower antiproliferative effect in non-malignant cells (IC_{50} values $\cong$ 30). In xenograft mouse models of ovarian cancer cells, by intraperitoneal administration, BBIT20 (**175**) displayed strong antitumour activity at very low concentration (2 mg kg^{-1}), being much more active than olaparib at 50 mg.kg^{-1}. Throughout the experiment, mice have not shown significant morbidity signs or alteration of body weight. In combination assays, BBIT20 (**175**) sensitized triple-negative breast and ovarian cancer cells to the effect of cisplatin and olaparib. Its synergy with these anticancer drugs was related to apoptosis induction.

Moreover, triple-negative breast and ovarian cancer cells did not develop resistance to BBIT20 (**175**) when exposed to several rounds of selection with increasing concentrations. Interestingly, BBIT20 (**175**) was previously found to be a strong P-gp inhibitor in resistant human *ABCB1*-gene transfected L5178Y mouse T-lymphoma cells (FAR 55.9 at 2 μM) (Paterna

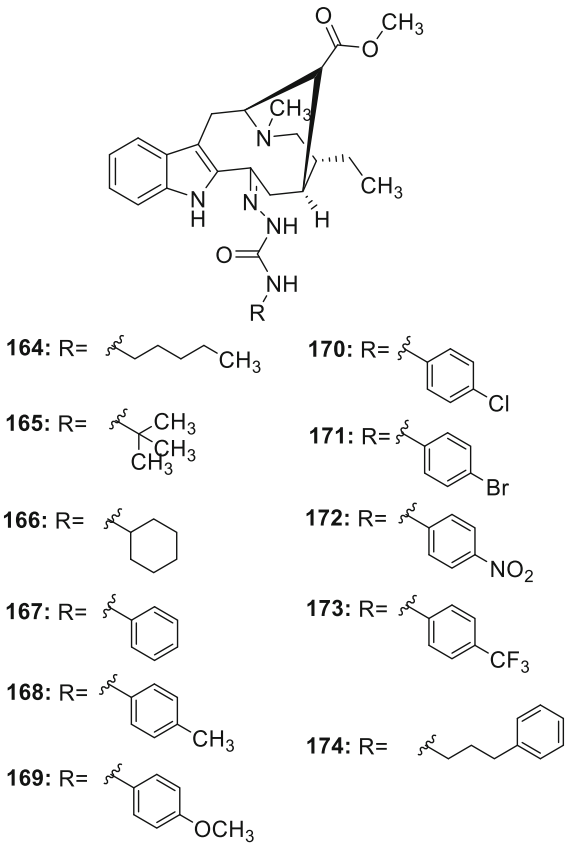


Fig. 21 Semicarbazone (**164**–**174**) dregamine derivatives

et al. 2017), thus corroborating its great potential for reversing drug-resistance. It was the first disrupter of BRCA1-BARD1 complex reported. As a single agent or in combination with anticancer drugs, namely PARP inhibitors, BBIT20 (**175**) is a promising lead for treating aggressive and resistant cancers, particularly triple-negative breast, and advanced ovarian cancer.

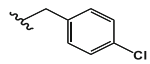
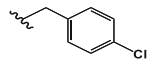
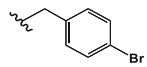
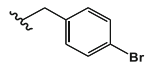
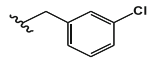
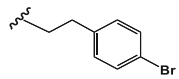
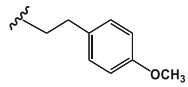
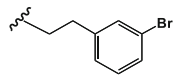
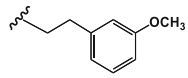
Other *Tabernaemontana* species

Tabernaemontana arborea

T. arborea ROSE ex J.D.SM., a shrub or small tree native to the tropical rainforests of Mexico, Central America, and Colombia, is used in Mexican traditional medicine due to their analgesic, anti-inflammatory, and dermatological properties (González-Trujano et al. 2023).

A bioassay-guided fractionation of the sap of this plant resulted in isolation of the known monoterpene indole alkaloid voacangine (**27**) (Fig. 6), along with the bisindole alkaloids voacamine (**176**) and epivoacorine (**177**) (Fig. 23). The cytotoxic activity of the three alkaloids was evaluated, and the half dose effect (ED_{50}) values in the P-388 lymphocytic leukaemia cells were 18.5 (**27**), 3.7 (**176**) and 2.4 (**177**) µM (Kingston 1978).

Table 11 P-gp inhibition of parental compounds tabernaemontanine (**117**) and dregamine (**118**) and the *N*-alkyl derivatives **125**–**128**, **134** and **141**–**144**, in human *ABCB1*-gene-transfected mouse lymphoma cells (Cardoso et al. 2021a)

Compound	R	Conc. µM	FAR[a]
117	**H**	2	0.99
		20	1.37
118	**H**	2	0.84
		20	1.53
125		2	11.73
		20	191.82
126		2	69.32
		20	203.23
127		2	55.75
		20	197.50
128		2	58.13
		20	203.66
134		2	40.00
		20	180.14
141		2	96.47
		20	193.40
142		2	26.17
		20	202.05
143		2	141.84
		20	279.43
144		2	37.45
		20	290.78
Verapamil[b]	–	20	6.60

[a]FAR–Fluorescence activity ratio: accumulation ratio of rhodamine 123 between resistant (MDR) and sensitive (PAR) cells. FAR > 1 means the compound is active; FAR > 10 means strong P-gp inhibition. [b]Verapamil was used as positive control

Tabernaemontana calcarea

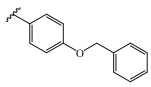
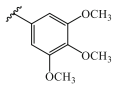
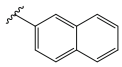
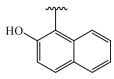
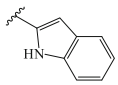
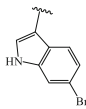
T. calcarea Pichon, also known as *Pandaca calcarea*, is a forest understory shrub predominantly found in the

Table 12 Dregamine azine (**147–156**) and semicarbazone (**165**, **166**) with sensitive collateral effect against resistant *ABCB1*-transfected (MDR) L5178Y mouse lymphoma cells (Cardoso et al. 2021b)

Compound	IC_{50} (μM)		RR[a]
	PAR Cells	MDR Cells	
147	14.80	5.96	0.40
149	13.05	4.62	0.35
151	14.46	6.57	0.45
153	23.66	8.40	0.36
155	26.40	7.75	0.29
156	18.08	8.64	0.48
165	26.27	12.33	0.47
166	12.85	5.69	0.44

[a]RR (Relative resistance ratio) = IC_{50}MDR/IC_{50}PAR; Selectivity against MDR cells: RR < 1; Collateral sensitivity effect: RR ≤ 0.5

Table 13 P-gp inhibition of the dregamine *azine* derivatives **158–163,** in human *ABCB1*-gene-transfected mouse lymphoma cells (Cardoso et al. 2021b)

Compound	R	Conc. μM	FAR[a]
158		0.2	3.50
		2	104.59
159		0.2	11.99
		2	100.07
160		0.2	30.74
		2	126.58
161		0.2	16.31
		2	128.48
162		0.2	6.07
		2	106.19
163		0.2	3.00
		2	95.56
Verapamil[b]	–	20	6.34

[a]FAR–Fluorescence activity ratio: accumulation ratio of rhodamine 123 between resistant (MDR) and sensitive (PAR) cells. FAR > 1 means the compound is active; FAR > 10 means strong P-gp inhibition. [b]Verapamil was used as positive control

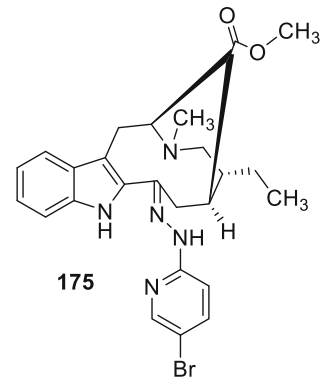


Fig.22 Chemical structure of BBIT20 (**175**)

western and northern regions of Madagascar. Three new indole alkaloids, 19-*epi*-3-oxovoacristine (**178**), 19-*epi*-coacristine hydroxyindoleine (**179**), and 3*R*/*S*-hydroxytabernanthine (**180**), along with the previously known indole alkaloids voacangine (**27**), isovoacangine (**181**), coronaridine (**182**), 11-hydroxycoronaridine (**183**), voacristine (**184**), 19-*epi*-voacristine (**185**), isovoacristine (**186**), ibogamine (**187**), 10-methoxyibogamine (**188**),heyneanine (**189**) and 19-*epi*-heyneanine (**190**) (Fig. 24), were isolated using a bioassay-guided fractionation. They were found to be marginally cytotoxic to ovarian cancer cells A2780, with IC_{50} values ranging from 12.5 to 28.6 μM (Chaturvedula et al. 2003).

Tabernaemontana inconspicua

T. inconspicua Stapf., a shrub known for its green to yellow or orange bark, is native to Africa and widely distributed across various tropical countries. This

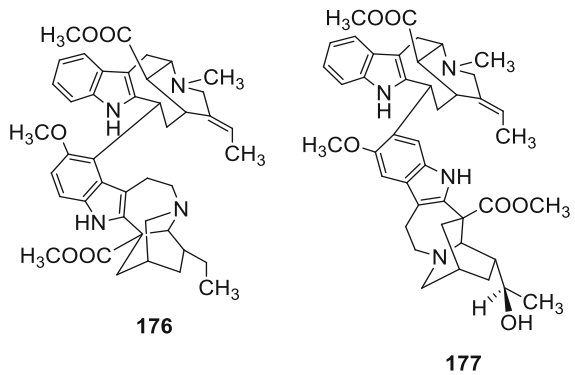
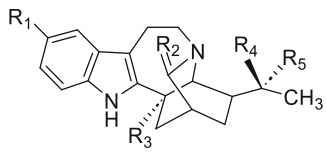
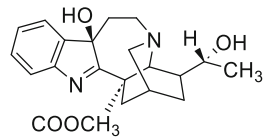


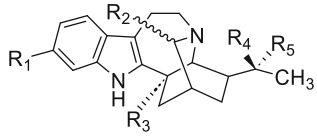
Fig. 23 Chemical structures of compounds **176** and **177** isolated from *T. arborea*



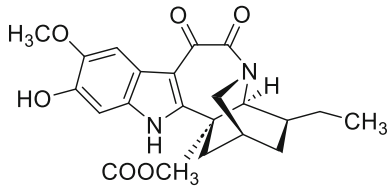
178: $R_1 = OCH_3$; $R_2 = O$; $R_3 = COOCH_3$; $R_4 = H$; $R_5 = OH$
27: $R_1 = OCH_3$; $R_2 = H_2$; $R_3 = COOCH_3$; $R_4 = R_5 = H$
182: $R_1 = R_4 = R_5 = H$; $R_2 = H_2$; $R_3 = COOCH_3$
184: $R_1 = OCH_3$; $R_2 = H_2$; $R_3 = COOCH_3$; $R_4 = OH$; $R_5 = H$
185: $R_1 = OCH_3$; $R_2 = H_2$; $R_3 = COOCH_3$; $R_4 = H$; $R_5 = OH$
187: $R_1 = R_3 = R_4 = R_5 = H$; $R_2 = H_2$
188: $R_1 = OCH_3$; $R_2 = H_2$; $R_3 = R_4 = R_5 = H$
189: $R_1 = R_3 = R_5 = H$; $R_2 = H_2$; $R_4 = OH$
190: $R_1 = R_3 = R_4 = H$; $R_2 = H_2$; $R_5 = OH$



179



180: $R_1 = OCH_3$; $R_2 = OH$; $R_3 = R_4 = R_5 = H$
181: $R_1 = OCH_3$; $R_2 = R_4 = R_5 = H$; $R_3 = COOCH_3$
183: $R_1 = OH$; $R_2 = R_4 = R_5 = H$; $R_3 = COOCH_3$
186: $R_1 = OCH_3$; $R_2 = R_5 = H$; $R_3 = COOCH_3$; $R_4 = OH$



191

Fig. 24 Chemical structures of compounds **178–186** isolated from *T. calcarea*

Fig. 25 Chemical structures of compound **191** isolated from *T. inconspicua*

species has received little research attention, and only a few studies have indicated the presence of indole alkaloids exhibiting cytotoxic effects (Ngah et al. 2022).

5,6-Dioxo-11-hydroxyvoacangine (**191**) (Fig. 25) inhibited the cell growth of human breast cancer MDA-MB-231 cells, with IC_{50} values after 24 h and 48 h of treatment of 3.35 and 2.19 μM, respectively (Laura et al. 2021).

Tabernaemontana pachysiphon

T. pachysiphon Stapf. is a perennial broad-leaved tree reaching up to 15 m and found in the coastal tropical lowland forests of East Africa. Root cortex decoctions are widely used in traditional African medicine, as they are believed to contain medicinal properties. Notably, *T. pachysiphon* is characterized by the presence of monoterpene indole alkaloids in all its parts (Höft et al. 1998). Phytochemical investigation of the leaves led to the isolation of 21 new bisindole alkaloids of the aspidosperma—aspidosperma type, including the new tabernaesines A − J (**192–200**), and the known 2′-hydroxyvoafoline (**201**) and isovoafolidine (**202**) (Fig. 26). Their cytotoxic activity was assessedon human cancer cell lines from, skin (SK-MEL-28), colon (SW480), liver (HepG2), breast (T47D and MDA-MB-231) and lung (A549), through the thiazolyl blue tetrazolium bromide assay. Tabernaesines A (**192**) and F (**197**), and 2′-hydroxyvoafoline (**201**) exhibited significant inhibitory effects on SK-MEL-28, SW480, HepG2, and T47D with IC_{50} values ranging from 2.5 to 9.8 μM. Tabernaesines E (**196**) and G (**198**) were also cytotoxic against some cancer cell lines (IC_{50} values ranging from 7.4 to 9.5 μM). Moreover, isovoafolidine (**202**) exhibited cytotoxicity to MDA-MB-231 cells (IC_{50} of 8.3 μM) (Yi et al. 2020).

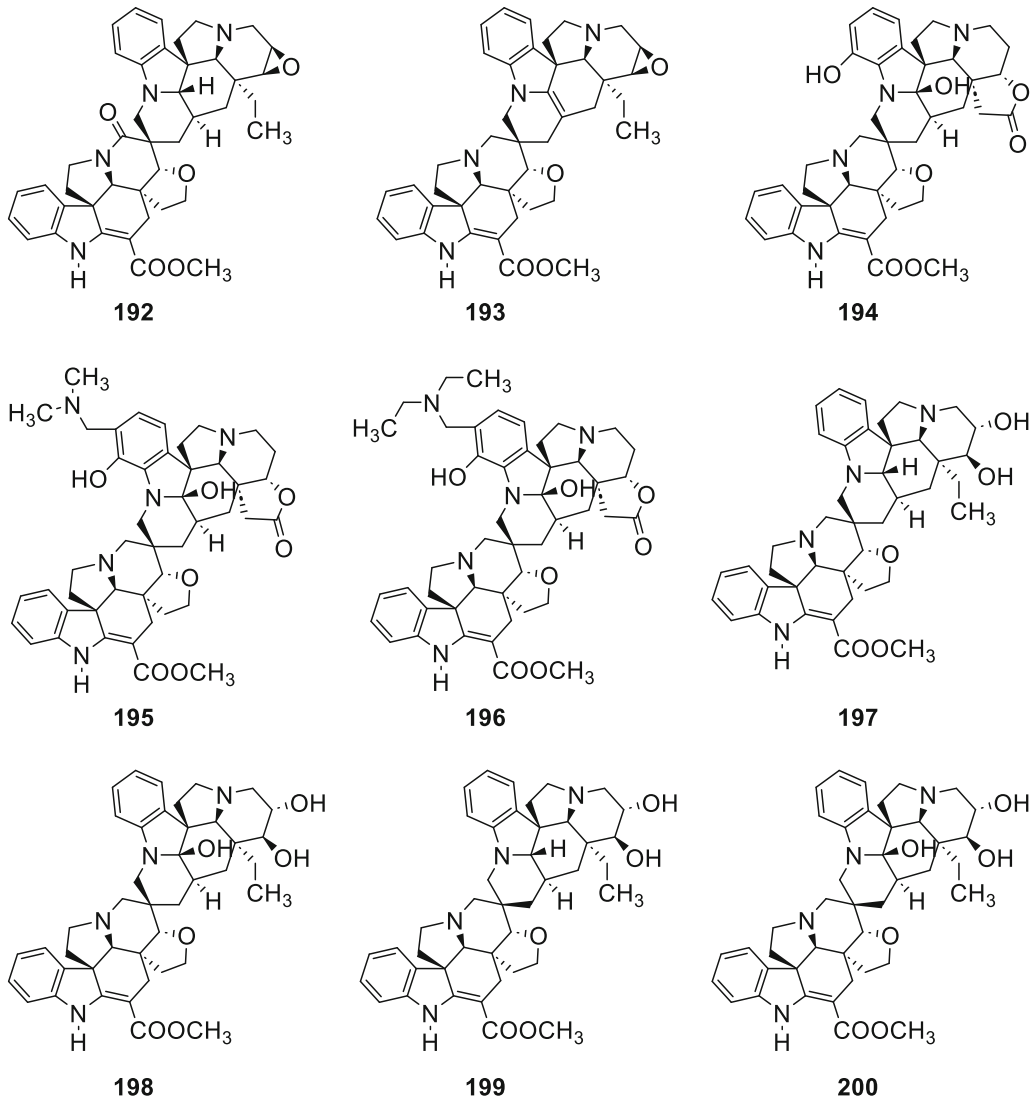


Fig. 26 Chemical structures of compounds **192–200** isolated from *T. pachysiphon*

Tabernaemontana sphaerocarpa

T. sphaerocarpa Blume is a small tree native to Indonesia and it is found mostly in Java. This species has several traditional uses, including the leaves used as a laxative, the flowers as a cardiotonic agent, and the latex has been applied for wart removal. Fractionation of the dichloromethane-soluble fraction of the methanol extract of *T. sphaerocarpa* stems gave rise to the isolation of two new bisindole alkaloids, biscarpamontamines A (**203**) and biscarpamontamine B (**204**), together with vobtusine (**205**), vobtusine lactone (**206**), and 3-hydroxyvobtusine (**207**) bisindole alkaloids (Fig. 27), which were evaluated for their cytotoxic activity against the human leukaemia (HL60), multiple myeloma (RPMI8226), lung cancer (NCI-H226), colon cancer (HCT116), and breast cancer (MCF7) cells. Among them, biscarpamontamine B (**204**), and 3-hydroxyvobtusine (**207**) exhibited the most significant cytotoxic effect with IC_{50} values ranging from 0.5 to 2.4 μM and 0.8–2.4 μM, respectively (Zaima et al. 2009).

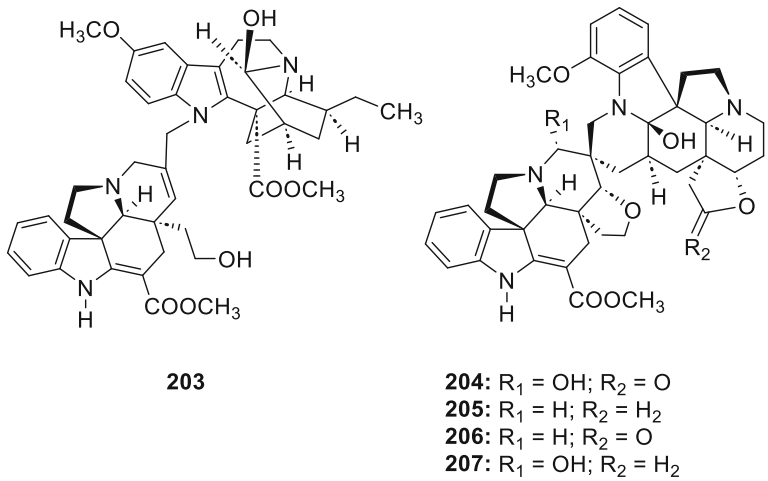


Fig. 27 Chemical structures of compounds **203–207** isolated from T. *sphaerocarpa*

Conclusions and future perspectives

Tabernaemontana species have long been used in traditional medicine to treat various diseases, including tumours. Their strong biological activity has been attributed mostly to the indole moiety of monoterpene indole and bisindole alkaloids. In fact, due to its chemical characteristics and biological properties, the indole nucleus has been considered a privileged scaffold in the development of anticancer drugs. It is found not only in plant-derived indole alkaloids in clinical use, such as vinblastine and vincristine, but also in several synthetic anticancer drugs. Thus, in the quest for new anticancer indole alkaloids, several researchers have been carrying out the phytochemical study of *Tabernaemontana* species.

The main objective of this review was to summarize these studies and to highlight our own contribution related to the study of *Tabernaemontana elegans*. A high number of monoterpene indole and alkaloids has been isolated and evaluated for their anticancer potential. Many compounds showed encouraging in vitro activity against sensitive and resistant phenotypes, through modulation of various signalling pathways, namely inhibition of cancer cell proliferation, cell cycle arrest, and apoptosis induction. The ability of monoterpene indole alkaloid derivatives, obtained by simple modifications of functional groups, to reverse multidrug resistance mediated by ABC transporters, mostly P-gp, has also been well documented by our group. The remarkable in vitro and in vivo results showed by the dregamine derivative BBIT20 (**175**), in triple-negative breast and ovarian cancers, strongly highlighted the importance of monoterpene indole alkaloids as leads in drug development. It revealed great potential for treating aggressive and resistant cancers directly or in combination with anticancer drugs currently in the frontline of BRCA-deficient tumours treatment.

Although a great number of studies has been reporting the anticancer properties of monoterpene indole alkaloids, in most cases the underlying mechanisms are often unclear or unexplored and should be thoroughly investigated. In addition to in vitro tests, in vivo studies should also be performed. They represent complex models that can address several issues that are not achievable through in vitro studies, namely, to evaluate the safety, toxicity, and efficacy of a lead compound and thus, together with in vitro studies provide a holistic understanding of the pharmacodynamic and pharmacokinetic profiles of lead compounds.

Acknowledgements The authors thank Fundação para a Ciência e a Tecnologia (FCT), Portugal, for financial support through the project 2022.05718.PTDC and PhD fellowship 2020.06020.BD (Filipa Barbosa).

Funding Open access funding provided by FCT|FCCN (b-on).

Data availability Not applicable.

Declarations

Conflict of interest The authors have no conflicts of interest to declare.

Open Access This article is licensed under a Creative Commons Attribution 4.0 International License, which permits use, sharing, adaptation, distribution and reproduction in any medium or format, as long as you give appropriate credit to the original author(s) and the source, provide a link to the Creative Commons licence, and indicate if changes were made. The images or other third party material in this article are included in the article's Creative Commons licence, unless indicated otherwise in a credit line to the material. If material is not included in the article's Creative Commons licence and your intended use is not permitted by statutory regulation or exceeds the permitted use, you will need to obtain permission directly from the copyright holder. To view a copy of this licence, visit http://creativecommons.org/licenses/by/4.0/.

References

Abubakar IB, Loh HS (2016) A review on ethnobotany, pharmacology and phytochemistry of Tabernaemontana corymbosa. J Pharm Pharmacol 68:423–432. https://doi.org/10.1111/jphp.12523

Abubakar IB, Lim KH, Kam TS, Loh HS (2016) Synergistic cytotoxic effects of combined δ-tocotrienol and jerantinine B on human brain and colon cancers. J Ethnopharmacol 184:107–118. https://doi.org/10.1016/j.jep.2016.03.004

Abubakar IB, Lim KH, Kam TS, Loh HS (2017) Enhancement of apoptotic activities on brain cancer cells via the combination of γ-tocotrienol and jerantinine A. Phytomedicine 30:74–84. https://doi.org/10.1016/j.phymed.2017.03.004

Alhuthali HM, Bradshaw TD, Lim KH et al (2020) The natural alkaloid Jerantinine B has activity in acute myeloid leukemia cells through a mechanism involving c-Jun. BMC Cancer 20:1–9. https://doi.org/10.1186/s12885-020-07119-2

Allen-Rhoades W (2024) A study to compare early use of vinorelbine and maintenance therapy for patients with high risk rhabdomyosarcoma. ClinicalTrials.gov. https://doi.org/10.1200/JCO.2022.40.16_suppl.TPS11591

Baassou S, Mehri H, Plat M (1978) Alcaloïds de Melodinus aeneus. Phytochemistry 17:1449–1450. https://doi.org/10.1016/S0031-9422(00)94618-1

Banyal A, Tiwari S, Sharma A et al (2023) Vinca alkaloids as a potential cancer therapeutics: recent update and future challenges. 3Biotech 13:1–17. https://doi.org/10.1007/s13205-023-03636-6

Bhadane BS, Patil MP, Maheshwari VL, Patil RH (2018) Ethnopharmacology, phytochemistry, and biotechnological advances of family Apocynaceae: a review. Phyther Res 32:1181–1210. https://doi.org/10.1002/ptr.6066

Binghe X (2019) Phase III study of vinflunine plus capecitabine versus capecitabine alone in patients with advanced breast cancer. ClinicalTrials.gov 10:524223

Cai YS, Sarotti AM, Zhou TL et al (2018) Flabellipparicine, a *Flabelliformide-apparicine*-type Bisindole alkaloid from *Tabernaemontana divaricata*. J Nat Prod 81:1976–1983. https://doi.org/10.1021/acs.jnatprod.8b00191

Cardoso DSP, Kincses A, Nové M et al (2021a) Alkylated monoterpene indole alkaloid derivatives as potent P-glycoprotein inhibitors in resistant cancer cells. Eur J Med Chem 210:112985. https://doi.org/10.1016/j.ejmech.2020.112985

Cardoso DSP, Szemerédi N, Spengler G et al (2021b) Exploring the monoterpene indole alkaloid scaffold for reversing p-glycoprotein-mediated multidrug resistance in cancer. Pharmaceuticals 14:862. https://doi.org/10.3390/PH14090862

Chaturvedula VSP, Sprague S, Schilling JK, Kingston DGI (2003) New cytotoxic indole alkaloids from *Tabernaemontana calcarea* from the Madagascar rainforest. J Nat Prod 66:528–531. https://doi.org/10.1021/np020548e

Chen J, Sun WL, Wasylyk B et al (2012) C-Jun N-terminal kinase mediates microtubule-depolymerizing agent-induced microtubule depolymerization and G2/M arrest in MCF-7 breast cancer cells. Anticancer Drugs 23:98–107. https://doi.org/10.1097/CAD.0b013e32834bc978

Chen J, Yu Y, Wu J et al (2021) Trimeric and dimeric Aspidosperma-type alkaloids from leaves of *Tabernaemontana divaricata* "Dwaft." Bioorg Chem 116:105314. https://doi.org/10.1016/j.bioorg.2021.105314

Chen SQ, Jia J, Hu JY et al (2022) Iboga-type alkaloids with Indolizidino[8,7-b]Indole scaffold and bisindole alkaloids from Tabernaemontana bufalina Lour. Phytochemistry 196:113089. https://doi.org/10.1016/j.phytochem.2022.113089

Chung FFL, Tan PFTM, Raja VJ et al (2017) Jerantinine A induces tumor-specific cell death through modulation of splicing factor 3b subunit 1 (SF3B1). Sci Rep 7:42504. https://doi.org/10.1038/srep42504

Dewick PM (2009) Medicinal natural products. A biosynthetic approach, 3rd edn. Wiley, Hoboken

Dey P, Kundu A, Kumar A et al (2020) Analysis of alkaloids (indole alkaloids, isoquinoline alkaloids, tropane alkaloids). Recent advances in natural products analysis. Elsevier, Amsterdam, pp 505–567

Du K, Li X, Zheng C et al (2023) Monoterpenoid indole alkaloid dimers from the *Melodinus axillaris* induce G2/M phase arrest and apoptosis via p38 MAPK activation in HCT116 cells. Bioorg Chem 140:106841. https://doi.org/10.1016/j.bioorg.2023.106841

Fang ZY, Ren YD, Du SY et al (2019) Melosuavine I, an apoptosis-inducing bisindole alkaloid from *Melodinus suaveolens*. Fitoterapia 133:175–179. https://doi.org/10.1016/j.fitote.2018.12.026

Fennell DA, Porter C, Lester J et al (2022) Active symptom control with or without oral vinorelbine in patients with relapsed malignant pleural mesothelioma (VIM): a randomised phase 2 trial. eClinicalMedicine 48:101432. https://doi.org/10.1016/j.eclinm.2022.101432

Fennell DA (2021) Vinorelbine in Mesothelioma (VIM). In: ClinicalTrials.gov

Ferreira M-JU, Paterna A (2019) Monoterpene indole alkaloids as leads for targeting multidrug resistant cancer cells from the African medicinal plant *Tabernaemontana elegans*. Phytochem Rev 18:971–987. https://doi.org/10.1007/s11101-019-09615-1

Feyzizadeh M, Barfar A, Nouri Z et al (2022) Overcoming multidrug resistance through targeting ABC transporters: lessons for drug discovery. Expert Opin Drug Discov 17:1013–1027. https://doi.org/10.1080/17460441.2022.2112666

PROTA Foundation (2008) Plant Resource of Tropical Africa (11)1 Medicinal Plants. PROTA Foundation

Frei R, Staedler D, Raja A et al (2013) Total synthesis and biological evaluation of jerantinine E. Angew Chemie - Int Ed 52:13373–13376. https://doi.org/10.1002/anie.201305533

Ge D, Tao HR, Fang L et al (2020) 11-Methoxytabersonine induces necroptosis with autophagy through AMPK/mTOR and JNK Pathways in human lung cancer cells. Chem Pharm Bull 68:244–250. https://doi.org/10.1248/cpb.c19-00851

Ghosh P, Poddar S, Chatterjee S (2021) Morphological features, phytochemical and ethnopharmacological attributes of *Tabernaemontana divaricata* Linn.: a comprehensive review. J Pharmacogn Phytochem 10:31–36. https://doi.org/10.22271/phyto.2021.v10.i6a.14253

González-Trujano ME, Páez-Martínez N, Krengel F et al (2023) Central nervous system activity of a *Tabernaemontana arborea* alkaloid extract involves serotonergic and opioidergic neurotransmission in murine models. Fitoterapia 169:1–8. https://doi.org/10.1016/j.fitote.2023.105602

Heffeter P, Pape VFS, Enyedy ÉA et al (2019) Anticancer thiosemicarbazones: chemical properties, interaction with iron metabolism, and resistance development. Antioxid Redox Signal 30:1062–1082. https://doi.org/10.1089/ars.2017.7487

Höft M, Verpoorte R, Beck E (1998) Growth and alkaloid patterns of roots of *Tabernaemontana pachysiphon* and *Rauvolfia mombasiana* as influenced by environmental factors. Bot Acta 111:222–230. https://doi.org/10.1111/j.1438-8677.1998.tb00699.x

Kam TS, Loh KY, Wei C (1993) Conophylline and conophyllidine: new dimeric alkaloids from *Tabernaemontana divaricata*. J Nat Prod 56:1865–1871. https://doi.org/10.1021/np50101a001

Kam T, Sim K, Koyano T, Komiyama K (1998) Conodiparines A-D, new bisindoles from cultured of vincristine-resistance. Bioorg Med Chem Lett 8:1693–1696. https://doi.org/10.1016/s0960-894x(98)00294-7

Kang J, Lewis TR, Gardner A et al (2022) Semi-Syntheses and interrogation of indole-substituted Aspidosperma terpenoid Alkaloids. Org Biomol Chem 20:3988–3997. https://doi.org/10.1039/x0xx00000x

Kingston DGI (1978) Plant anticancer agents VI: isolation of voacangine, voacamine, and epivoacorine from Tabernaemontana arborea sap. J Pharm Sci 67:271–272. https://doi.org/10.1002/jps.2600670242

Laura GFM, Njoya EM, Jouda JB et al (2021) A new cytotoxic indole alkaloid from *Tabernaemontana inconspicua* stapf. Nat Prod Res 35:1590–1595. https://doi.org/10.1080/14786419.2019.1628749

Lim KH, Hiraku O, Komiyama K, Kam TS (2008) Jerantinines A-G, cytotoxic Aspidosperma alkaloids from *Tabernaemontana corymbosa*. J Nat Prod 71:1591–1594. https://doi.org/10.1021/np800435c

Lim KH, Raja VJ, Bradshaw TD et al (2015) Ibogan, tacaman, and cytotoxic bisindole alkaloids from *Tabernaemontana. Cononusine*, an iboga alkaloid with unusual incorporation of a pyrrolidone moiety. J Nat Prod 78:1129–1138. https://doi.org/10.1021/acs.jnatprod.5b00117

Lim SM, Mohamad Hanif EA, Chin SF (2021) Is targeting autophagy mechanism in cancer a good approach? The possible double-edge sword effect. Cell Biosci 11:56. https://doi.org/10.1186/s13578-021-00570-z

Liu Y-P, Li Y, Cai X-H et al (2012) Melodinines M−U, cytotoxic alkaloids from *Melodinus suaveolens*. J Nat Prod 75:220–224. https://doi.org/10.1021/np2009169

Liu ZW, Zhang J, Li ST et al (2018) Ervadivamines A and B, two unusual trimeric Monoterpenoid indole alkaloids from *Ervatamia divaricata*. J Org Chem 83:10613–10618. https://doi.org/10.1021/acs.joc.8b01371

Low YY, Lim KH, Choo YM et al (2010) Structure, biological activity, and a biomimetic partial synthesis of the lirofolines, novel pentacylic indole alkaloids from Tabernaemontana. Tetrahedron Lett 51:269–272. https://doi.org/10.1016/j.tetlet.2009.10.122

Ma K, Wang JS, Luo J et al (2014) Tabercarpamines A-J, apoptosis-inducing indole alkaloids from the leaves of *Tabernaemontana corymbosa*. J Nat Prod 77:1156–1163. https://doi.org/10.1021/np401098y

Marinho FF, Simões AO, Barcellos T, Moura S (2016) Brazilian *Tabernaemontana genus*: indole alkaloids and phytochemical activities. Fitoterapia 114:127–137. https://doi.org/10.1016/j.fitote.2016.09.002

Ngah L, Tsopgni WDT, Nyobe JCN et al (2022) A New Antimicrobial Phenylpropanol from the Leaves of *Tabernaemontana inconspicua* Stapf. (Apocynaceae) Inhibits Pathogenic Gram-Negative bacteria. Antibiotics 11:1–7. https://doi.org/10.3390/antibiotics11010121

Nge CE, Sim KS, Lim SH et al (2016) A Hexacyclic, Ibogaderived Monoterpenoid indole with a contracted tetrahydroazepine C-Ring and incorporation of an Isoxazolidine moiety, a Seco-corynanthean, an Aspidosperma-aspidosperma bisindole with anticancer properties, and the absolute configuratio. J Nat Prod 79:2709–2717. https://doi.org/10.1021/acs.jnatprod.6b00674

O'Connor SE, Maresh JJ (2006) Chemistry and biology of monoterpene indole alkaloid biosynthesis. Nat Prod Rep 23:532–547. https://doi.org/10.1039/b512615k

Paterna A, Borralho PM, Gomes SE et al (2015) Monoterpene indole alkaloid hydrazone derivatives with apoptosis inducing activity in human HCT116 colon and HepG2 liver carcinoma cells. Bioorganic Med Chem Lett 25:3556–3559. https://doi.org/10.1016/j.bmcl.2015.06.084

Paterna A, Kincses A, Spengler G et al (2017) Dregamine and tabernaemontanine derivatives as ABCB1 modulators on resistant cancer cells. Eur J Med Chem 128:247–257. https://doi.org/10.1016/j.ejmech.2017.01.044

Paterna A, Khonkarn R, Mulhovo S et al (2018) Monoterpene indole alkaloid azine derivatives as MDR reversal agents. Bioorganic Med Chem 26:421–434. https://doi.org/10.1016/j.bmc.2017.11.052

Pluchino KM, Hall MD, Goldsborough AS et al (2012) Collateral sensitivity as a strategy against cancer multidrug resistance. Drug Resist Updat 15:98–105. https://doi.org/10.1016/j.drup.2012.03.002

Pratchayasakul W, Pongchaidecha A, Chattipakorn N, Chattipakorn S (2008) Ethnobotany and ethnopharmacology of *Tabernaemontana divaricata*. Indian J Med Res 127:317–335

Qazzaz ME, Raja VJ, Lim KH et al (2016) In vitro anticancer properties and biological evaluation of novel natural alkaloid jerantinine B. Cancer Lett 370:185–197. https://doi.org/10.1016/j.canlet.2015.10.013

Raimundo L, Paterna A, Calheiros J et al (2021) BBIT20 inhibits homologous DNA repair with disruption of the BRCA1–BARD1 interaction in breast and ovarian cancer. Br J Pharmacol 178:3627–3647. https://doi.org/10.1111/bph.15506

Raja VJ, Lim KH, Leong CO et al (2014) Novel antitumour indole alkaloid, Jerantinine A, evokes potent G2/M cell cycle arrest targeting microtubules. Invest New Drugs 32:838–850. https://doi.org/10.1007/s10637-014-0126-1

Reis FL, Adolpho L, Ruiz ALTG et al (2022) In vitro antiproliferative activity of alkaloids isolated from *Tabernaemontana catharinensis* A.DC (Apocynaceae). Nat Prod Res 36:5808–5812. https://doi.org/10.1080/14786419.2021.2017928

Rosales PF, Marinho FF, Gower A et al (2019) Bio-guided search of active indole alkaloids from *Tabernaemontana catharinensis*: Antitumour activity, toxicity in silico and molecular modelling studies. Bioorg Chem 85:66–74. https://doi.org/10.1016/j.bioorg.2018.12.016

Silvestri R (2013) New prospects for vinblastine analogues as anticancer agents. J Med Chem 56:625–627. https://doi.org/10.1021/jm400002j

Sim DSY, Teoh WY, Sim KS et al (2016) Vobatensines A-F, Cytotoxic Iboga-Vobasine Bisindoles from *Tabernaemontana corymbosa*. J Nat Prod 79:1048–1055. https://doi.org/10.1021/acs.jnatprod.5b01117

Sim DSY, Navanesan S, Sim KS et al (2019) Conolodinines A-D, Aspidosperma- Aspidosperma Bisindole Alkaloids with Antiproliferative Activity from *Tabernaemontana corymbosa*. J Nat Prod 82:850–858. https://doi.org/10.1021/acs.jnatprod.8b00919

Smedley CJ, Stanley PA, Qazzaz ME et al (2018) Sustainable Syntheses of (-)-Jerantinines A & e and Structural Characterisation of the Jerantinine-Tubulin Complex at the Colchicine Binding Site. Sci Rep 8:10617. https://doi.org/10.1038/s41598-018-28880-2

Song J, Zhang B, Li M, Zhang J (2023) The current scenario of naturally occurring indole alkaloids with anticancer potential. Fitoterapia 165:105430. https://doi.org/10.1016/j.fitote.2023.105430

Van Beek TA, Verpoorte R, Svendsen AB et al (1984) *Tabernaemontana L.*: a review of its Taxonomy, Phytochemistry Ethnobotany and Pharcology. J Ethnopharmacol 10:113–138

Xu J, Qu W, Cao WY et al (2019) Chemical constituents from *Tabernaemontana bufalina* Lour. Chem Biodivers 16:12–17. https://doi.org/10.1002/cbdv.201800491

Yi WF, Ding X, Chen YZ et al (2020) Tabernaesines A-I, cytotoxic Aspidosperma-Aspidosperma-Type Bisindole alkaloids from *Tabernaemontana pachysiphon*. J Nat Prod 83:3215–3222. https://doi.org/10.1021/acs.jnatprod.9b00768

Yu Y, Wu J, Bao MF et al (2023) Diverse aspidosperma-type alkaloids from the leaves of *Tabernaemontana bovina* with anti-hepatoma activity. Fitoterapia 169:105588. https://doi.org/10.1016/j.fitote.2023.105588

Yuan YX, Zhang Y, Guo LL et al (2017) Tabercorymines A and B, Two Vobasinyl-Ibogan-Type Bisindole alkaloids from *Tabernaemontana corymbosa*. Org Lett 19:4964–4967. https://doi.org/10.1021/acs.orglett.7b02445

Zaima K, Hirata T, Hosoya T et al (2009) Biscarpamontamines A and B, an aspidosperma-iboga bisindole alkaloid and an aspidosperma-aspidosperma bisindole alkaloid, from *Tabernaemontana sphaerocarpa*. J Nat Prod 72:1686–1690. https://doi.org/10.1021/np900365r

Zhang BJ, Teng XF, Bao MF et al (2013) Cytotoxic indole Alkaloids from *Tabernaemontana divaricata*. J Nat Prod 75:1406–1412. https://doi.org/10.1021/np400130y

Zhang BJ, Teng XF, Bao MF et al (2015a) Cytotoxic indole alkaloids from *Tabernaemontana officinalis*. Phytochemistry 120:46–52. https://doi.org/10.1016/j.phytochem.2014.12.025

Zhang Y, Guo L, Yang G et al (2015b) New vobasinyl-ibogan type bisindole alkaloids from *Tabernaemontana corymbosa*. Fitoterapia 100:150–155. https://doi.org/10.1016/j.fitote.2014.11.016

Zhang BJ, Lu JS, Bao MF et al (2018a) Bisindole alkaloids from *Tabernaemontana corymbosa*. Phytochemistry 152:125–133. https://doi.org/10.1016/j.phytochem.2018.04.020

Zhang Y, Yuan YX, Goto M et al (2018b) Taburnaemines A-I, Cytotoxic Vobasinyl-Iboga-Type Bisindole Alkaloids from *Tabernaemontana corymbosa*. J Nat Prod 81:562–571. https://doi.org/10.1021/acs.jnatprod.7b00949.MS

Zhang Y, Ding X, Yuan YX et al (2020) Cytotoxic Monoterpenoid Indole Alkaloids from *Tabernaemontana corymbosa* as potent autophagy inhibitors by the attenuation of lysosomal acidification. J Nat Prod 83:1432–1439. https://doi.org/10.1021/acs.jnatprod.9b00856

Zhou SY, Zhou TL, Qiu G et al (2018) Three New cytotoxic Monoterpenoid Bisindole alkaloids from *Tabernaemontana bufalina*. Planta Med 84:1127–1133. https://doi.org/10.1055/a-0608-4988

Publisher's Note Springer Nature remains neutral with regard to jurisdictional claims in published maps and institutional affiliations.